AD-A068 220 PURDUE RESEARCH FOUNDATION LAFAYETTE IND F/G 9/5
THE EFFECTS OF SUBSTRATE COMPOSITION ON THICK FILM CIRCUIT RELI--ETC(U)
FEB 79 R W VEST N00019-78-C-0236
UNCLASSIFIED NL

| OF |
ADA
068220

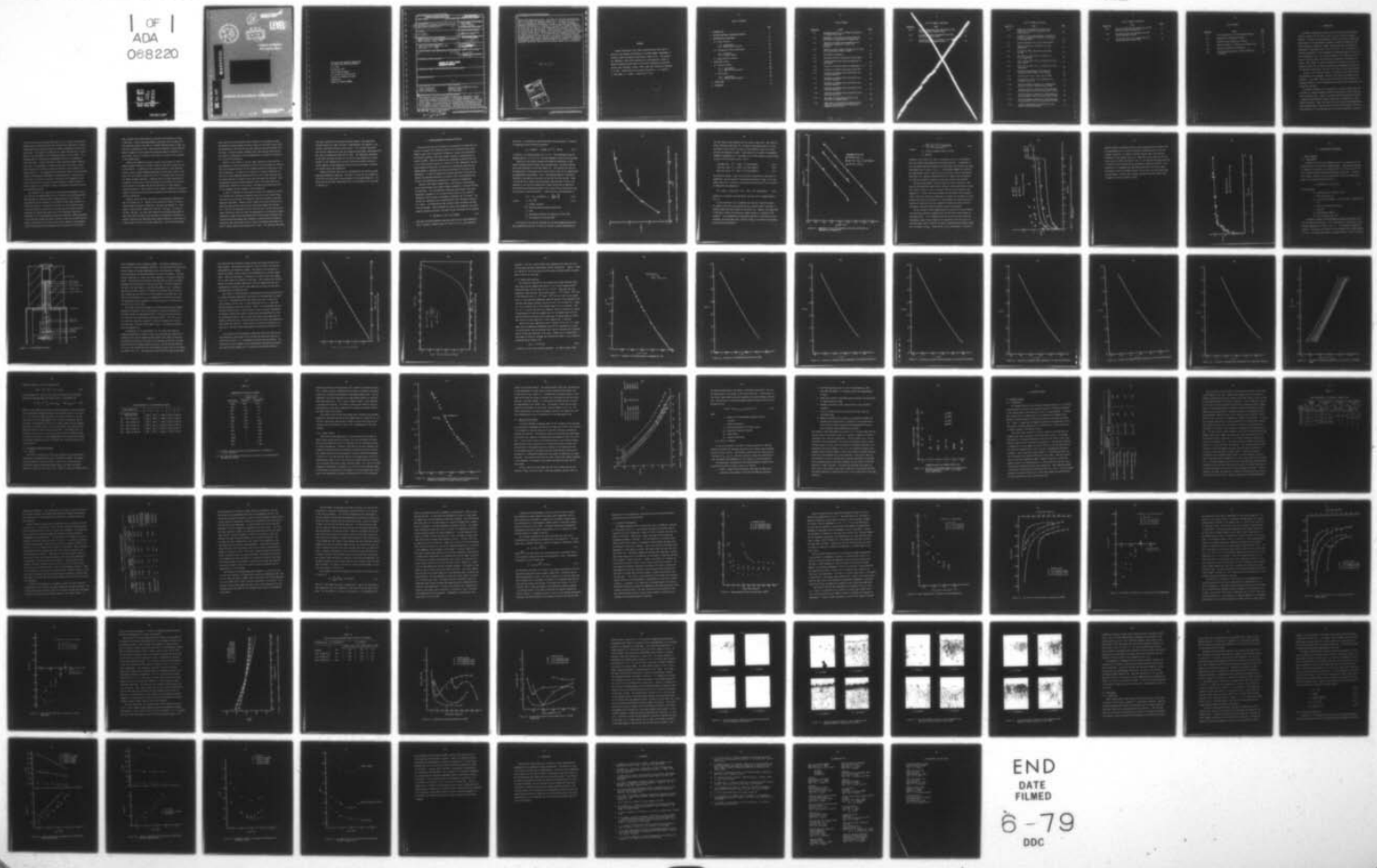

END
DATE FILMED
6-79
DDC

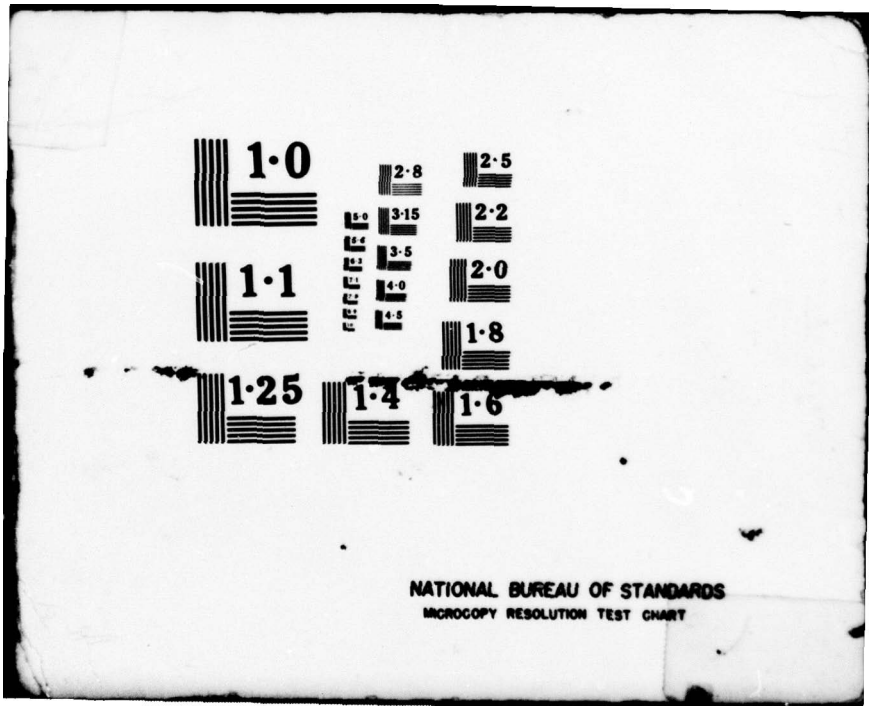
1·0
1·1
1·25
2·8
3·15
3·5
4·0
4·5
1·4
2·5
2·2
2·0
1·8
1·6
NATIONAL BUREAU OF STANDARDS
MICROCOPY RESOLUTION TEST CHART

PURDUE UNIVERSITY
West Lafayette, Indiana

SCHOOL OF MATERIALS ENGINEERING

THE EFFECTS OF SUBSTRATE COMPOSITION ON THICK FILM CIRCUIT RELIABILITY

R. W. Vest

28 February 1979

Final Technical Report

For the period 2/1/78-1/31/79

Contract No. N00019-78-C-0236

Prepared for

NAVAL AIR SYSTEMS COMMAND

SECURITY CLASSIFICATION OF THIS PAGE (When Data Entered)

REPORT DOCUMENTATION PAGE

READ INSTRUCTIONS BEFORE COMPLETING FORM

1. REPORT NUMBER
2. GOVT ACCESSION NO.
3. RECIPIENT'S CATALOG NUMBER

4. TITLE (and Subtitle)
(6) THE EFFECTS OF SUBSTRATE COMPOSITION ON THICK FILM CIRCUIT RELIABILITY.

5. TYPE OF REPORT & PERIOD COVERED
Final Report
2/1/78 - 1/31/79

6. PERFORMING ORG. REPORT NUMBER

7. AUTHOR(s)
(10) R. W. Vest

8. CONTRACT OR GRANT NUMBER(s)
(15) N00019-78-C-0236

9. PERFORMING ORGANIZATION NAME AND ADDRESS
PURDUE RESEARCH FOUNDATION, ~~PURDUE UNIVERSITY~~
West Lafayette, Indiana 47907

10. PROGRAM ELEMENT, PROJECT, TASK AREA & WORK UNIT NUMBERS
(12) 91p.

11. CONTROLLING OFFICE NAME AND ADDRESS
(11) NAVAL AIR SYSTEMS COMMAND, AIR 310B
Washington, D. C. 20361

12. REPORT DATE
28 Feb 1979

13. NUMBER OF PAGES
81

14. MONITORING AGENCY NAME & ADDRESS (if different from Controlling Office)
(9) Final rept. 1 Feb '78 - 31 Jan 79

15. SECURITY CLASS. (of this report)
Unclassified

15a. DECLASSIFICATION/DOWNGRADING SCHEDULE
N/A

16. DISTRIBUTION STATEMENT (of this Report)

APPROVED FOR PUBLIC RELEASE:
DISTRIBUTION UNLIMITED

17. DISTRIBUTION STATEMENT (of the abstract entered in Block 20, if different from Report)

18. SUPPLEMENTARY NOTES

19. KEY WORDS (Continue on reverse side if necessary and identify by block number)

Thick Film Resistors
Ceramic Substrates
Electrical Resistivity
Temperature Coefficient Resistivity
Electronic Glass
Glass Sintering

20. ABSTRACT (Continue on reverse side if necessary and identify by block number)

The saturation solubility of AlSiMag 614 (96% Al_2O_3) substrates in thick film resistor glass was determined as a function of temperature. These results were combined with dissolution rate studies in order to test various kinetic models. The viscosity of the resistor glass was measured as a function of amount of dissolved AlSiMag 614 substrate from the softening point to the annealing point of the glasses. The isothermal viscosity was found to increase by a factor of 20 with 10w/o dissolved substrate relative to the

DD FORM 1 JAN 73 1473 EDITION OF 1 NOV 65 IS OBSOLETE
S/N 0102-014-6601

SECURITY CLASSIFICATION OF THIS PAGE (When Data Entered)

Jcd

Jcd 291600

standard lead borosilicate glass. The affects of the minor constitutients (4%) in the AlSiMag 614 substrate composition on viscosity and surface tension of the glasses was determined to be small. The sheet resistance, temperature dependence of resistance, and the current noise were measured for thick film resistors as a function of the amount of substrate dissolved in the resistor for various firing temperatures at constant firing time, and for various firing times at 800°C. Large variations in these three properties were observed, and the changes were qualitatively correlated with changes in viscosity of the glass. The microstructure development and charge transport models used to correlate the results indicate a retardation of microstructure development in the resistors as the amount of dissolved substrate increases which brings about changing proportions of sintered and nonsintered contacts in the RuO_2 networks within the body of the resistor. Preliminary results on MIM devices fabricated with resistor glasses are also presented.

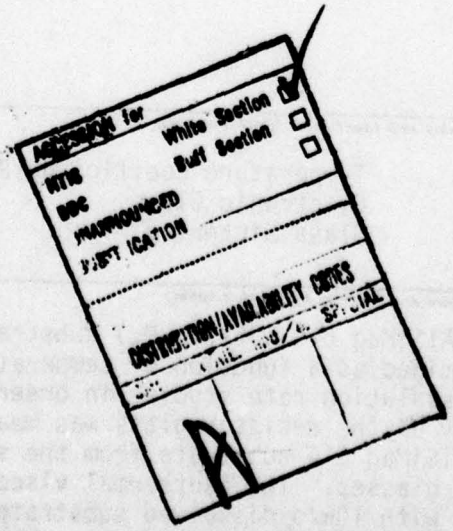

FOREWORD

Research described in this report constitutes the third year of effort on this program for the Naval Air Systems Command, Department of the Navy, under the technical cognizance of James Willis. The research was conducted in the Turner Laboratory for Electroceramics, School of Materials Engineering and School of Electrical Engineering, Purdue University, West Lafayette, Indiana 47907, under the direction of Professor R. W. Vest. Contributing to the project were Messrs. J. M. Himelick, P. Palanisamy, R. L. Reed, D. Tandan and C-T Tarn.

TABLE OF CONTENTS

LIST OF FIGURES

LIST OF FIGURES (Continued)

LIST OF FIGURES (Continued)

LIST OF FIGURES (Continued)

LIST OF TABLES

1. INTRODUCTION

The ceramic substrate upon which thick film circuits are printed and fired is a carrier for the circuit, but it is also a source of reactive material. The print and fire processing of thick film circuits ensures that there always will be some degree of chemical interaction between the film and the substrate, because all common substrate materials are soluble to some degree in the glasses used in thick film inks. This interaction is primarily responsible for the development of adhesion between the thick film and the substrate, but it also leads to changes in the composition of the glass with the net result that the physical properties of the glass will change. These changes in physical properties of the glass will result in modified kinetics for the various microstructure development processes and all electrical properties of resistors are related to their microstructure.

The goal of this research program is to develop a sufficient level of understanding of the phenomena involved so that appropriate models can be developed. These models should lead to the writing of specifications for substrate chemistry, and to recommendations concerning glass composition and processing conditions.

The Turner Laboratory for Electroceramics at Purdue University has been involved in a research program on conduction mechanisms in thick film resistors for several years. Some of the results have been published [1-4] and a summary of the pertinent findings through 1975 is presented in a final report to ARPA [5]. One of the results of this study was the demonstration that the glass plays a variety of roles in thick film resistors. One function certainly is to provide adhesion to the ceramic substrate, but even in

this case the results have shown that there is not a simple glass-substrate bonding layer but rather that the glass dissolves the substrate to an appreciable depth and the substrate material diffuses throughout the resistor to some extent. The research at Purdue has also shown that the glass is instrumental in the development of the conducting network in the resistor. The proposed model for microstructure development consists of a sequence of steps involving: 1) glass sintering; 2) glass spreading between conductive particles; 3) rearrangement of conductive particles in the glass; 4) glass densification; 5) sintering of conductive particles; and 6) growth of conductive particles. The parameters which affect the kinetics of the different stages of microstructure development include wettability, surface tension of the glass, viscosity of the glass, solubility of the conductive in the glass, particle size of the glass and the conductive, volume fraction of glass to conductive, uniformity of mixing, and chemical reactions involving the ingredient materials.

The influence of the substrate on microstructure development in thick film resistors was demonstrated by X-ray diffraction line broadening experiments designed to study the growth of RuO_2 particles in the resistor. It was observed that the presence of an AlSiMag 614 (96% Al_2O_3) substrate inhibited the increase in crystallite size after an initial rapid increase. X-ray phase analysis results did not indicate any new crystalline phases formed due to interactions between any of the ingredients (RuO_2-glass-substrate) for the time-temperature conditions employed in these experiments. It was found that alumina was readily soluble in the glass at 800^oC and this change in composition of the glass could lead to changes in the parameters controlling microstructure development such as wettability of the glass to

RuO_2, viscosity and surface tension of the glass, and solubility of RuO_2 in the glass. Contact angle measurements using glass with ten weight percent substrate material dissolved in it showed complete wetting to RuO_2, but the rate of spreading was less. Data from the isothermal shrinkage measurements on compacts of glass powder with substrate material dissolved in it gave surface tension to viscosity ratios lower by a factor of four compared to the standard glass.

Another role played by the glass in thick film resistors is that of a charge transport medium for a certain fraction of the total current carried by the resistor. In addition to well sintered contacts in the conducting network, certain contacts between conducting oxide particles contain a thin glass film and transport through this film in an important part of the overall charge transport mechanism. Properties such as voltage coefficient of resistance, current noise, stability and short time overload are very sensitively related to the number and the characteristics of these contacts. Electrical behavior of such contacts is very strongly related to the impurity content of the glass and hence would be expected to be sensitive to substrate-resistor interactions.

Progress during the first two years of this program was summarized in two final reports [6, 7]. Studies of the dissolution kinetics of two different alumina substrates (AlSiMag 614 - 96% Al_2O_3 and AlSiMag 772 - 99.5% Al_2O_3) in two base glass compositions (63% PbO - 25% B_2O_3 - 12% SiO_2 and 70% PbO - 20% B_2O_3 - 10% SiO_2) were conducted by performing experiments in which the change in weight of the substrate or the amount of substrate dissolved in the glass was determined after complete immersion in the glass for a known length of time at a constant temperature. Of the three mechanisms

which could limit the dissolution rate of alumina in the presence of glass, the molecular diffusion model was found to apply for the 63-25-12 glass while the dissolution in the 70-20-10 glass was limited by the phase boundary reaction rate. Diffusion through a boundary layer under natural convection was not found to be important for the time-temperature relationships characteristic of thick film processing.

Studies of the kinetics of initial stage sintering of glass particles were conducted in order to determine the ratio of surface tension to viscosity for the two standard glasses, and the standard glasses with additions of substrate ingredients. The data for all glasses fit a model of Newtonian viscous flow as the predominant mechanism for the initial stage sintering, and the surface tension to viscosity ratios were calculated from the data. Both the magnitude and the activation energies of this ratio were found to be significantly different for the glasses, confirming the extreme sensitivity of this parameter to small changes in glass composition.

In order to determine to what extent the electrical properties of thick film resistors are affected by substrate dissolution in the resistor glass, resistors with known amounts of AlSiMag 614 substrate dissolved in the glass phase were fabricated. Changes in glass composition during firing were prevented by screen printing and firing on substrates wrapped with platinum foil. The foil was separated from the fired resistors, and the devices were either fitted with electrical leads for measurements or sintered onto ceramic substrates in order to give more mechanical strength before attaching leads. Current-voltage measurements were conducted on several devices sintered to substrates, and linear behavior over 6 orders of magnitude using either forward or reverse polarity was observed in all cases. The resistors fabricated

from glass containing 10% dissolved substrate showed a room temperature resistance which was higher by factor of approximately 100 compared to the resistors fabricated with pure 63-25-12 glass. All resistors fabricated from the 10% substrate glass were very stable and gave highly reproducable TCR data over the temperature range -55^{o} to $125^{o}C$. The temperature dependence of the sheet resistance relative to its value at room temperature was much greater for the standard glass resistors, and they exhibited a much more erratic behavior during temperature cycling with the resistance increasing very sharply below room temperature.

Research during the past year has concentrated on the resistor system RuO_2-glass-AlSiMag 614 substrate. The glass frit used was the standard 63-25-12 glass with and without varying amounts of dissolved AlSiMag 614. The effects due to the minor constituents (4%) in the AlSiMag 614 are discussed in Section 3.2.

2. RESISTOR-SUBSTRATE INTERACTION KINETICS

Previous studies [7] of the kinetics of dissolution of AlSiMag 614 substrates in resistor films containing the 63-25-12 lead borosilicate glass showed a rapid initial dissolution followed by a slower rate during which the substrate content of the glass reached a maximum in approximately 10 minutes at 840°C. Empirical equations were developed to describe the kinetics of the dissolution process as a function of time, temperature, and substrate content in the glass, but there was an uncertainty concerning the maximum amount of substrate which could be dissolved in the glass at any temperature. In order to develop more accurate equations to describe the kinetics of substrate dissolution in resistor films, the saturation solubility of the substrate was determined as a function of temperature.

Resistor films (95w/o standard glass + 5w/o RuO_2) of approximately 25 μm fired thickness were screen printed on weighed, 2.5 cm square AlSiMag 614 substrates. The film-substrate system was equilibrated at the given temperature, quenched in air to avoid reprecipitation of any substrate ingredients from the glass, and weighed to determine the film weight. The resistor was decomposed using concentrated HCl under ultrasonic agitation for 3 hours. The substrate was then rinsed in water followed by acetone, dried and weighed. From the weight loss (Δw) of the substrate, the weight percent substrate dissolved in the glass (p) was calculated by the equation

$$P = 100\ \Delta w/(\Delta w + 0.95 \times \text{film weight}) \qquad (2.1)$$

Runs with increasing exposure times were carried out at each temperature until P reached a constant value; this value of P is P_o, the saturation

solubility. The solubility results were empirically expressed as a function of temperature by the following expression

$$P_o = 0.34634\ T - 1.45299 \times 10^{-4}\ T^2 - 187.89 \qquad (2.2)$$

in which P_o is in weight percent and T is in K. The experimental data are compared with Eq. 2.2 in Fig. 2.1, and the agreement is seen to be quite good.

Results for the surface recession of AlSiMag 614 substrates in bulk glasses (standard 63-25-12 glass, 5w/o substrate glass, and 10w/o substrate glass) were presented in an earlier report [7]. The recession was found to be proportional to the square root of time at short times for all compositions and temperatures investigated. This is the expected behavior if molecular diffusion of the species in the glass is the rate limiting step [8]. Starting with the Fick's second law and assuming a constant molar volume of the substrate in all the glass compositions, Cooper [8] derived an expression for diffusion controlled mass transport into a glass from a semi-infinite slab for the case of a moving interface. A modified form of that expression is:

$$f(\alpha) = \sqrt{\pi}\ \alpha\ \exp(\alpha^2)\mathrm{erfc}\ \alpha \cong -\left[\frac{P_o - P}{100 - P}\right] \qquad (2.3)$$

in which

$$\alpha = y/2\sqrt{D^* t} \qquad (2.4)$$

y = surface recession

D^* = effective binary diffusion coefficient

t = time

P_o = saturation solubility of substrate in glass (w/o)

P = w/o substrate in the bulk glass

The values of $f(\alpha)$ can be calculated for any given temperature and bulk glass composition using Eqs. 2.2 and 2.3, and the α values corresponding to

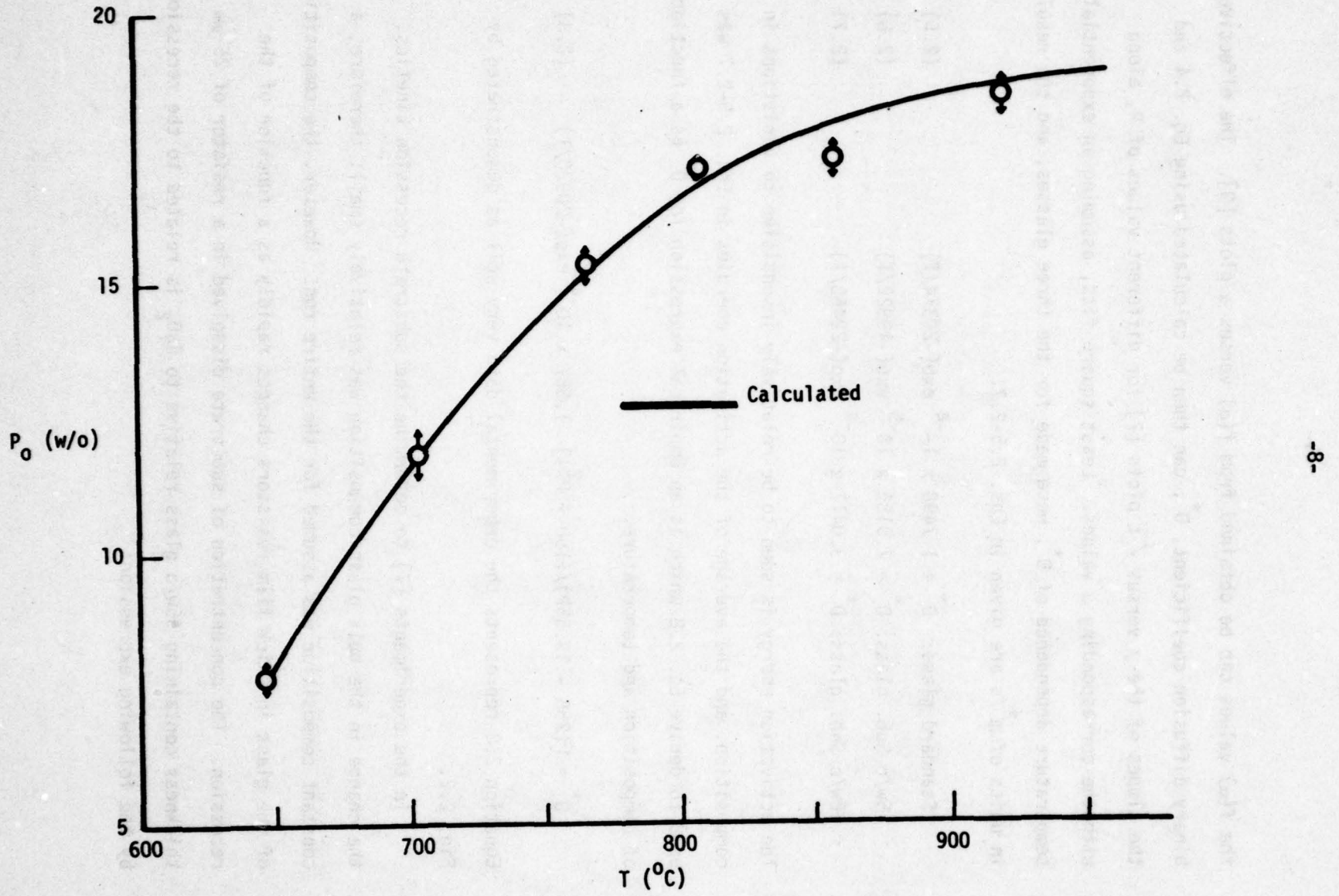

Figure 2.1. Saturation Solubility of AlSiMag 614 Substrate in Standard Glass Film.

the $f(\alpha)$ values can be obtained from $f(\alpha)$ versus α plots [9]. The effective binary diffusion coefficient, D^*, can then be calculated using Eq. 2.4 and the slopes of the y versus $\sqrt{t}$ plots [7] for different values of P, along with the corresponding α values. Least square fits, assuming an exponential temperature dependence of D^*, were made for the three glasses, and the results in units of m^2/s are given in Eqs. 2.5-2.7.

$$\text{Standard glass: } D^* = 1.7498 \times 1^{-4} \exp(-20374/T) \tag{2.5}$$

$$\text{5w/o Sub. glass: } D^* = 7.9185 \times 10^{-5} \exp(-19922/T) \tag{2.6}$$

$$\text{10w/o Sub. glass: } D^* = 3.0417 \times 10^{-4} \exp(-22463/T) \tag{2.7}$$

The activation energy is seen to be relatively insensitive to variations in composition, and the average of the activation energies in Eqs. 2.5-2.7 was used to derive Eq. 2.8 which is an empirical expression for D^* as a function of composition and temperature.

$$D^* = [(258 - 13.55P)/(150 + P^2)] \; 1.667 \times 10^{-4} \exp(-20920/T) \tag{2.8}$$

Equation 2.8 represents the experimental data very well as demonstrated by Fig. 2.2.

In the experiments [7] to determine the substrate recession kinetics, the change in the bulk glass composition was relatively small; therefore, a constant composition was assumed for the entire run. However, the composition of the glass in thick film resistors changes rapidly as a function of the recession. The concentration of substrate dissolved in a resistor of 25 μm thickness containing 95w/o glass relative to RuO_2 is related to the recession by the following expression:

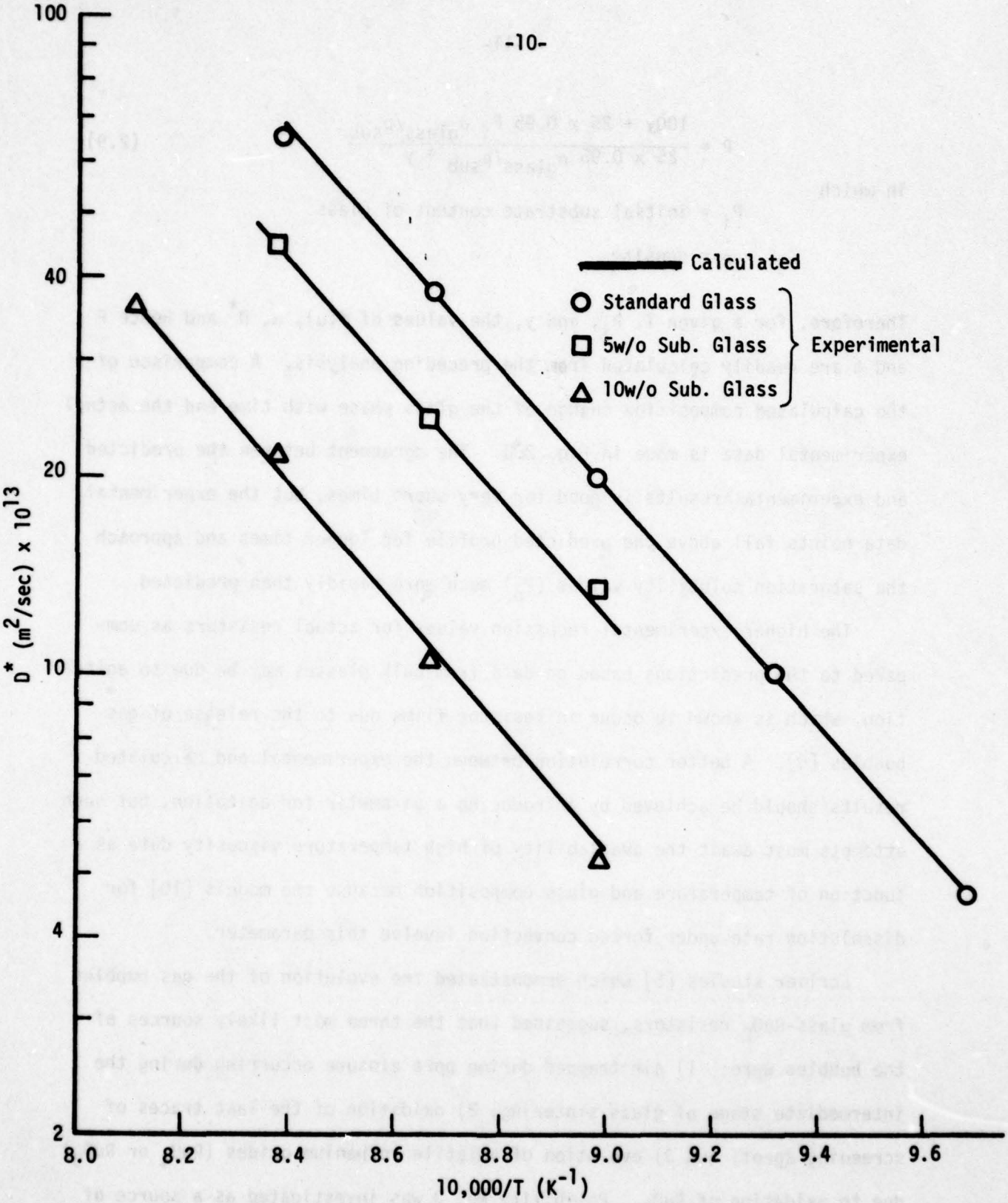

Figure 2.2. Dependence of the Effective Binary Diffusion Coefficient on Temperature and Composition.

$$P = \frac{100y + 25 \times 0.95\ P_i\ \rho_{glass}/\rho_{sub}}{25 \times 0.95\ \rho_{glass}/\rho_{sub} + y} \qquad (2.9)$$

in which

P_i = initial substrate content of glass

ρ = density

Therefore, for a given T, P_i, and y, the values of $f(\alpha)$, α, D^* and hence P and t are readily calculated from the preceding analysis. A comparison of the calculated composition change of the glass phase with time and the actual experimental data is made in Fig. 2.3. The agreement between the predicted and experimental results is good for very short times, but the experimental data points fall above the predicted profile for longer times and approach the saturation solubility values (P_o) much more rapidly than predicted.

The higher experimental recession values for actual resistors as compared to the predictions based on data from bulk glasses may be due to agitation, which is known to occur in resistor films due to the release of gas bubbles [5]. A better correlation between the experimental and calculated results should be achieved by introducing a parameter for agitation, but such attempts must await the availability of high temperature viscosity data as a function of temperature and glass composition because the models [10] for dissolution rate under forced convection involve this parameter.

Earlier studies [5] which demonstrated the evolution of the gas bubbles from glass-RuO_2 resistors, suggested that the three most likely sources of the bubbles were: 1) air trapped during pore closure occurring during the intermediate stage of glass sintering; 2) oxidation of the last traces of screening agent; and 3) evolution of volatile ruthenium oxides (RuO_4 or RuO_3) due to oxidation of RuO_2. Posibility No. 3 was investigated as a source of

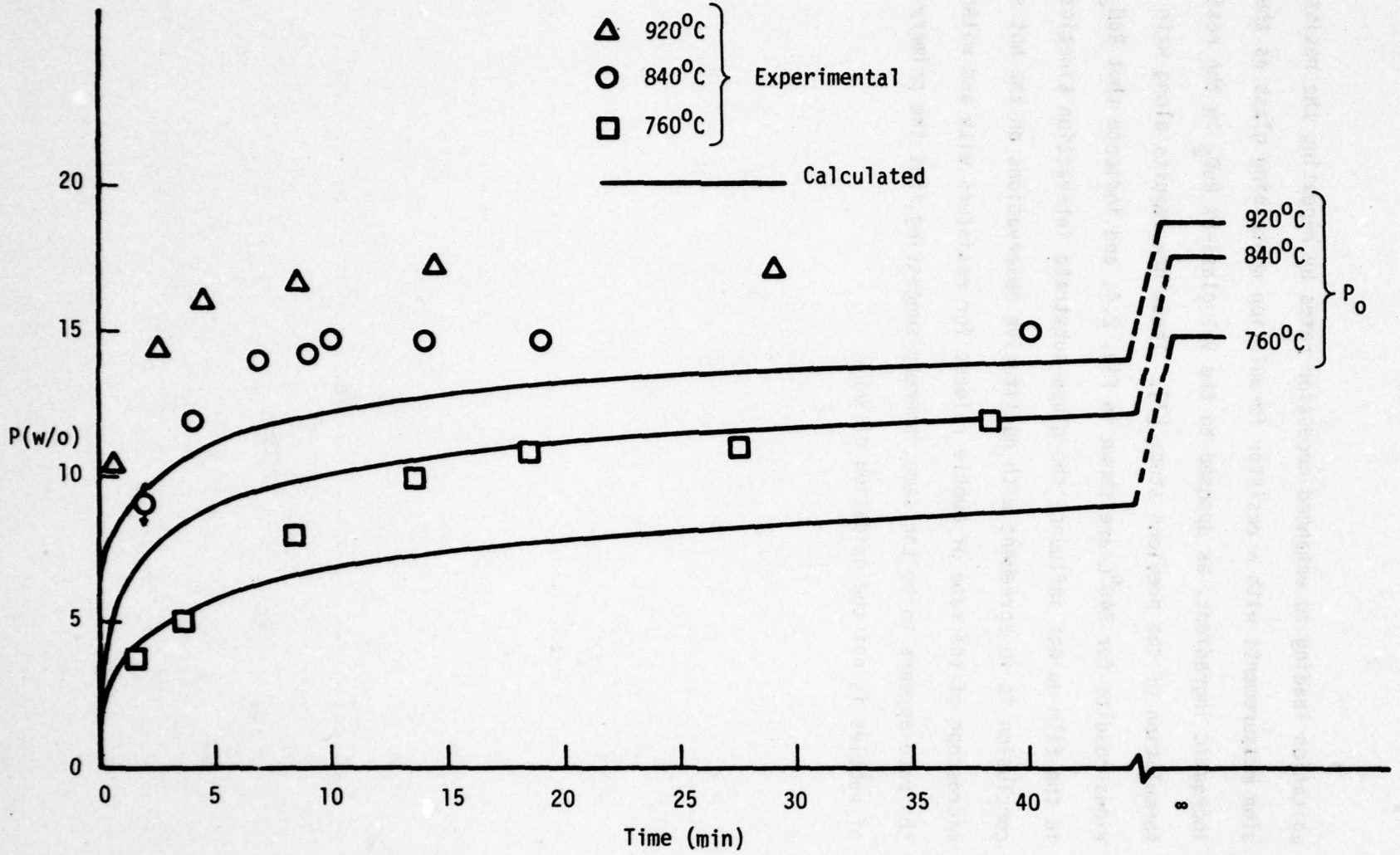

Figure 2.3. Comparison of Theory and Experiment for Dissolution of AlSiMag 614 in Thick Film Resistors.

agitation leading to enhanced recession rates by repeating the resistor recession measurements with a resistor formulation containing glass as the only inorganic ingredient, as opposed to the 95% glass-5% RuO_2 in the resistor formulation of the previous study [7]. These new results along with the previous results for 840^{o}C are shown in Fig. 2.4, and indicate that RuO_2 particles in the film do not influence the glass-substrate interaction kinetics. This conclusion is in agreement with qualitative observations on the hot stage microscope of the rate of bubble release for resistors with and without RuO_2; the rate appears to be the same, thereby suggesting that the primary source of bubbles is not the oxidation of RuO_2.

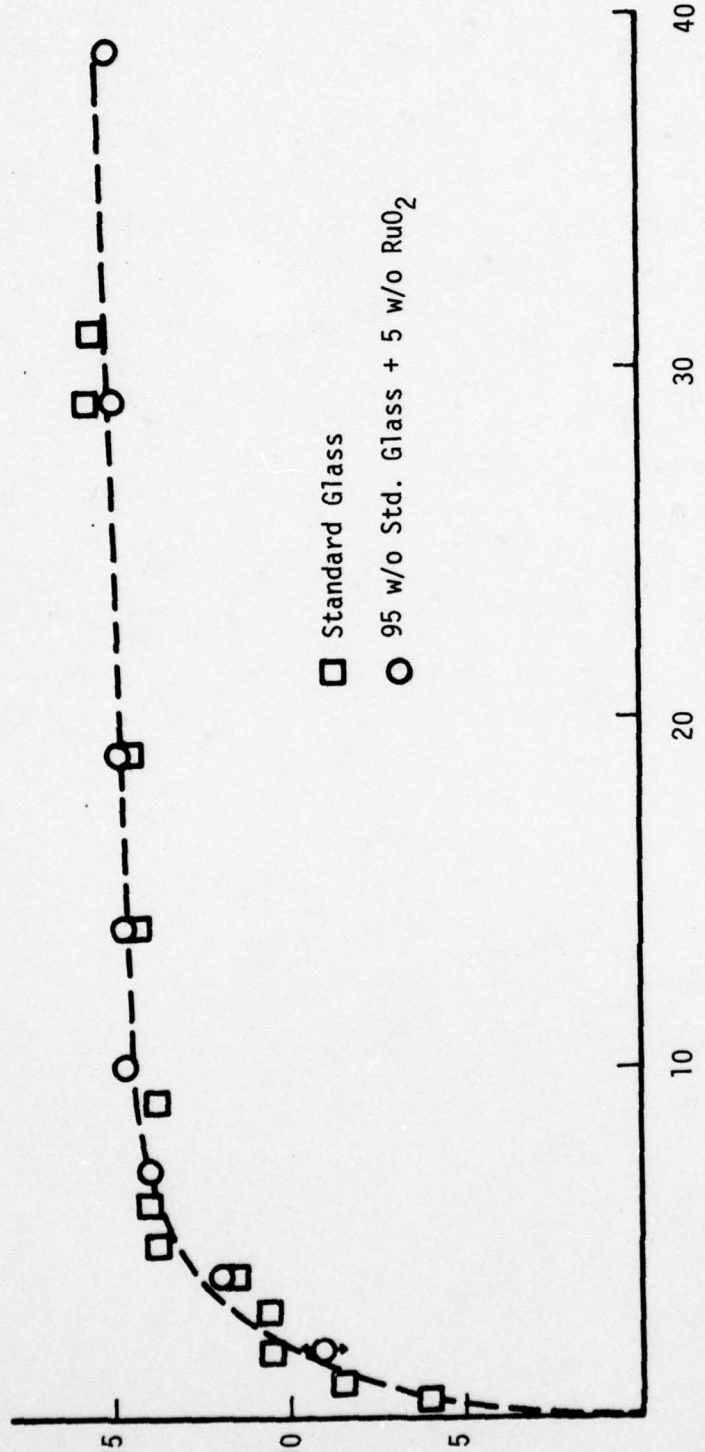

Figure 2.4. Kinetics of Glass Composition Variation in Glass Films and Resistor Films at 840°C.

3. MICROSTRUCTURE DEVELOPMENT

3.1 Glass Viscosity

3.1.1 Experimental

Trouton[11] was the first researcher to derive an expression for the viscous traction of horizontally supported beams. Experimental techniques for determinig viscosities in the range of 10^8 to 10^{15} poise (10^7 to 10^{14} Pa·s) by measuring beam bending were described by Hagy [12]. A modified form of Hagy's expression for the viscosity of a centrally loaded beam in terms of its mid-point deflection rate is:

$$\eta = (g\ell^3/144I_c v)[L + (\rho_g A/1.6)] \qquad (3.1)$$

In this equation:

g = acceleration due to gravity, cm/s^2

ℓ = free span length, cm

I_c = cross sectional moment of inertia (width x thickness^3/12), cm^4

v = mid-point deflection rate, cm/s

L = load, gm

ρ_g = glass density, gm/cm^3

A = cross sectional area, cm^2

A schematic diagram of the beam bending viscometer developed to measure the mid-point deflection, v, of a glass beam as a function of time at elevated temperatures is shown in Fig. 3.1. The viscometer assembly was housed in a clam sheel tube furnace 10 cm in diameter with a heated length of 60 cm. The furance was mounted on a wheeled support so that it could be

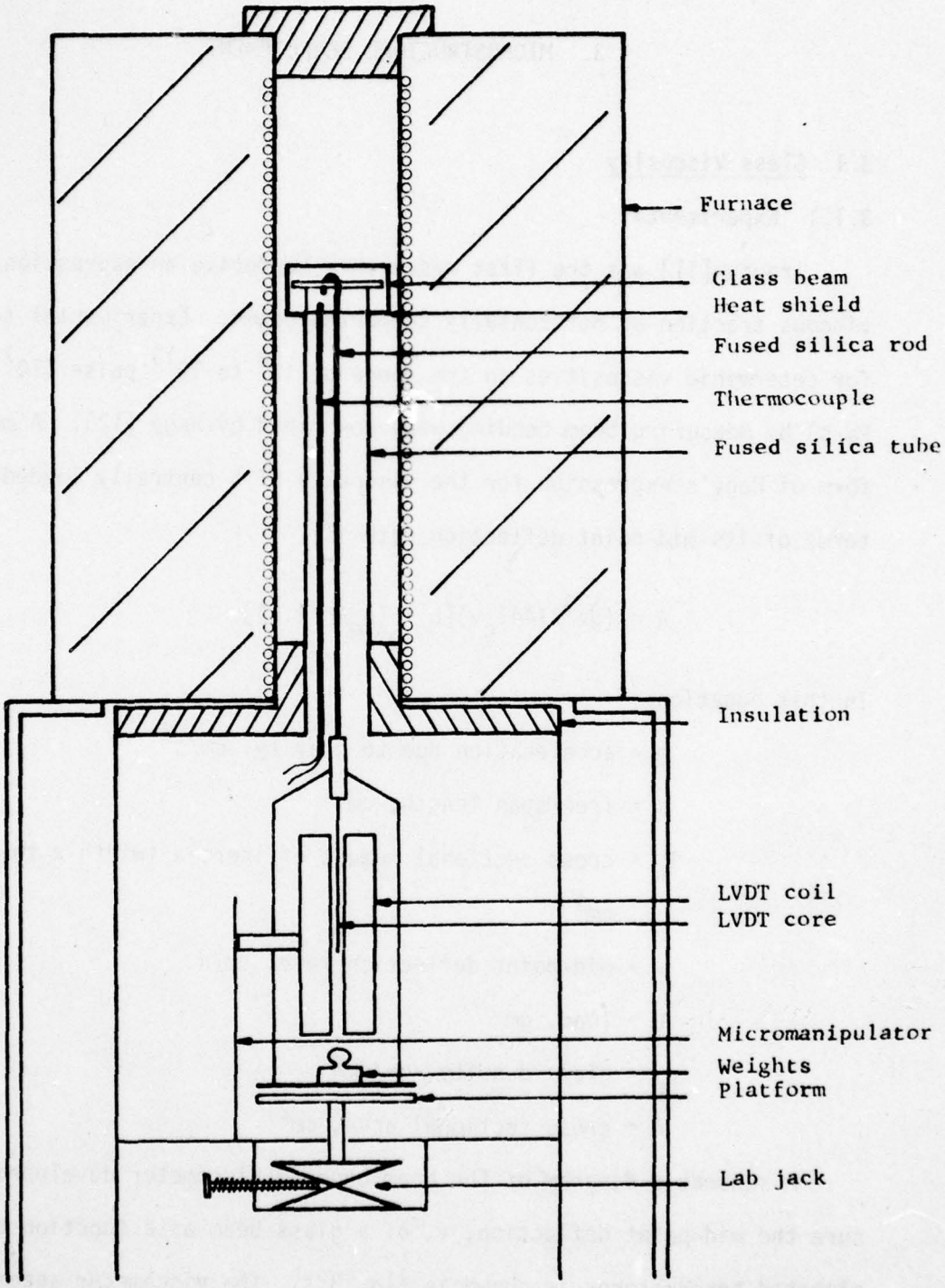

Figure 3.1. Beam Bending Viscometer.

moved independent of the viscometer assembly. The furnace temperature was controlled by an SCR programmable controller. The stainless steel heat shield served to equalize the beam temperature, which was measured by a chromel-alumel thermocouple located approximately 5 mm from the specimen. The glass beam was supported on a fused silica tube cemented to a tripod with leveling screws. Two platinum strips placed on the tube under the ends of the beam prevented the glass beam from sticking to the tube. The inner diameter of the tube is the span length, L, once the beam begins to sag. A load was applied to the beam by means of a fused silica rod with a hook at one end and a weights pan and the core of an LVDT cemented to the other end. The LVDT coil was mounted on an x-y-z micromanipulator resting on the tripod. The weights pan could be supported or relased by means of a lab jack which was also fixed to the tripod.

The glasses with varying amounts of dissolved substrate were prepared according to procedures, and in the apparatus, previously described [7]. The molten glasses at approximately 800^{o}C in platinum crucibles were cast in a stainless steel mold held at approximately 200^{o}C. The 7 cm x 5 cm x 1 cm slabs were annealed, and beams of required thickness was sliced off the slab using a low speed diamond wheel cutter. The beams were polished with 6 μm diamond grit.

In preparation for an experimental run, the fused silica tube was plumbed by adjusting the leveling screws, the glass beam was placed on the platinum strips, and the loading rod was placed at the center of the beam. The horizontal position of the LVDT coil was adjusted so that the core hung free inside the coil without touching the walls, and the vertical position of the coil was adjusted until the core reached the upper limit of the operating range of the coil. The furance was closed around the support tube making

sure that there was no physical contact between the furnace and the viscometer assembly. The furance was heated at a rate of $3^{o}C$/min, and the platform supporting the weight was lowered. The output of the LVDT went to a digital volt meter, and the output of the thermocouple to a digital thermometer. These two instruments, in addition to a digital clock, were imaged with a video camera and recorded on video tape. This procedure was followed because all three variables (deflection, time, and temperature) had to be simultaneously recorded, and the video camera was available and provided a convenient means to accomplish this.

The linearity of the system was investigated by measuring the deflection of a beam at constant temperature; the results of this experiment are shown in Fig. 3.2. The deflection rate (the slope of the line) is seen to be quite constant, and this rate, v, when substituted in Eq. 3.1 along with the beam constants, gives the viscosity. After it was established that the mid-point deflection was a linear function of time at constant temperature, the program controller was used to increase the beam temperature at a rate of approximately $3^{o}C$/min, and the video tape record used to determine the change in deflection over a 20 second time span during which the temperature would change less than $1^{o}C$. Typical results for mid-point deflection as a function of time under increasing temperature conditions are shown in Fig. 3.3

The stability of the viscometer assembly was checked by replacing the glass beam with a thick fused silica rod, and the system was found to be stable even at $600^{o}C$, i.e., no apparent beam deflection was measured. The reliability of the viscometer and the experimental technique was evaluated by using Viscosity Standard No. 711 supplied by the National Bureau of

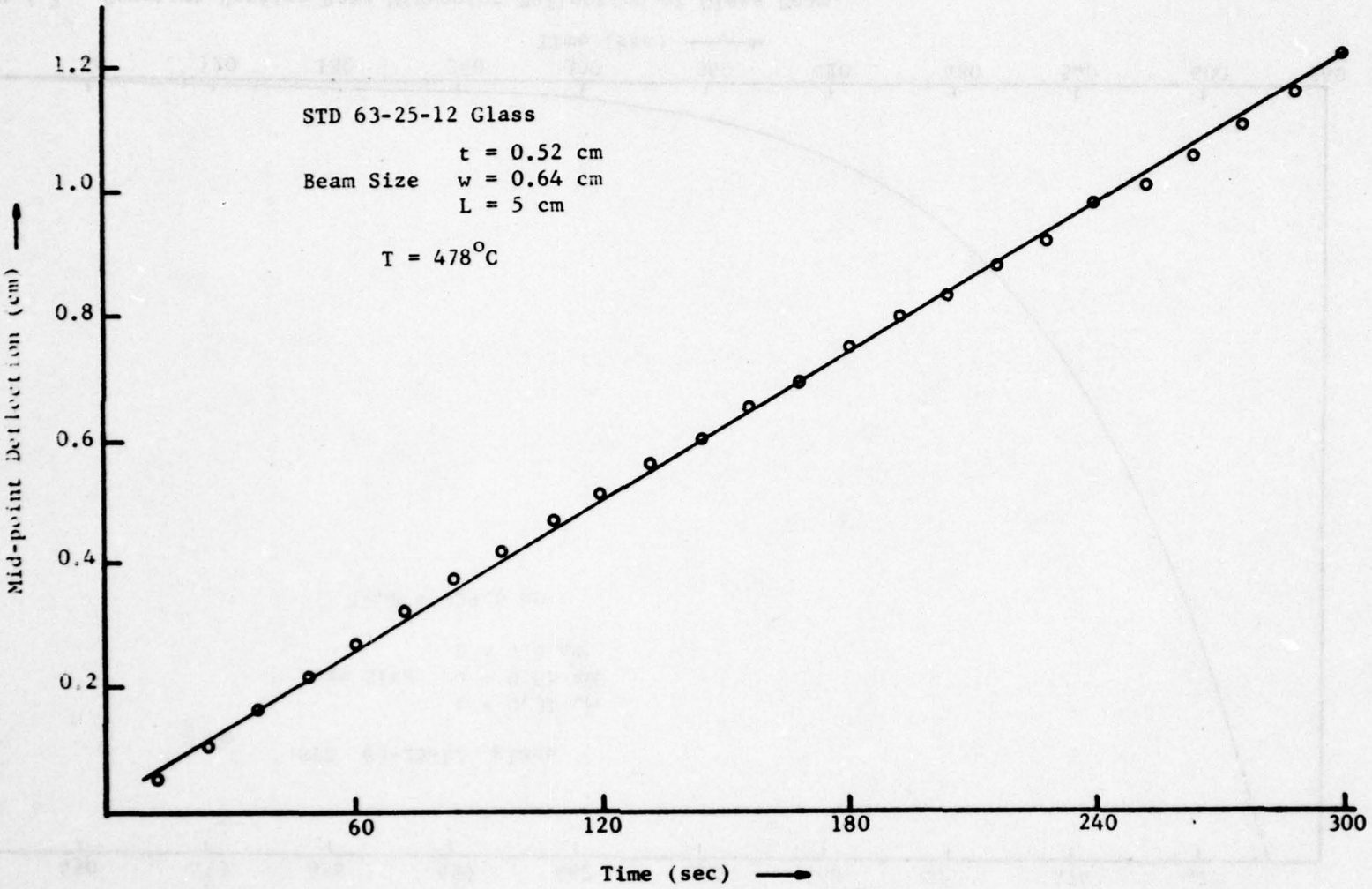

Figure 3.2. Isothermal Mid-point Deflection of Glass Beam.

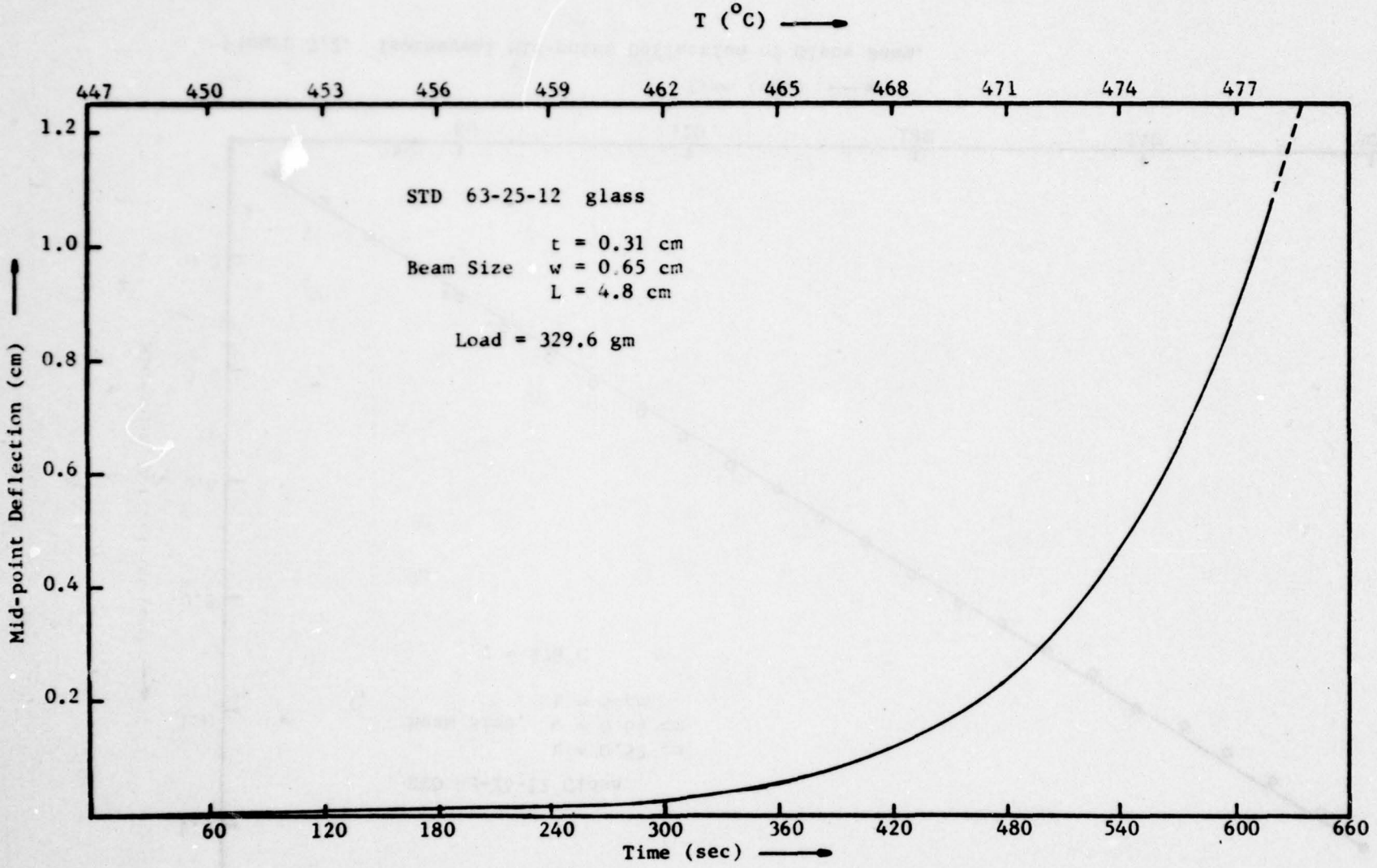

Figure 3.3. Constant Heating Rate Mid-point Deflection of Glass Beam.

Standards. This was a lead silicate glass composition for which the viscosity has been precisely established by several laboratories. Figure 3.4 shows our results for this glass along with the values predicted by NBS; the agreement is seen to be very good.

3.1.2 Results and Discussion

The viscosities obtained for the standard glass (63w/o PbO-25w/o B_2O_3-12w/o SiO_2) and the standard glass with 2, 4, 6, 8 and 10 weight percent dissolved AlSiMag 614 are shown in Figs. 3.5-3.10. These data span the temperature range from near the softening point ($\eta = 10^{7.6}$ poise = $10^{6.6}$ Pa·s) to the annealing point ($\eta = 10^{13}$ poise = 10^{12} Pa·s) for each of the glasses. This is a very important temperature range for several of the important microstructure development processes occuring in thick film resistors [5]. Figure 3.11 is an Arrhenius plot of the viscosity data for all six glasses. From Fig. 3.11, it can be seen that the isothermal viscosity increases by a factor of approximately 20 from the standard glass to the standard glass with 10 percent dissolved substrate, and an approximate 20 degree spread for equivalent viscosity values among the six glass compositions is observed.

None of the glass compositions gave a straight line on Fig. 3.11, which means that the temperature dependence could not be represented by a single activation energy, and the deviation from linearity increases with increasing amount of dissolved substrate in the glass. Another way of representing a wide range of viscosity, although not theoretically sound, is by an empirical expression due to Fulcher [13]:

$$\log \eta = A + B/(T-T_o) \qquad (3.2)$$

in which A, B, and T_o are arbitrary constants. In order to apply linear

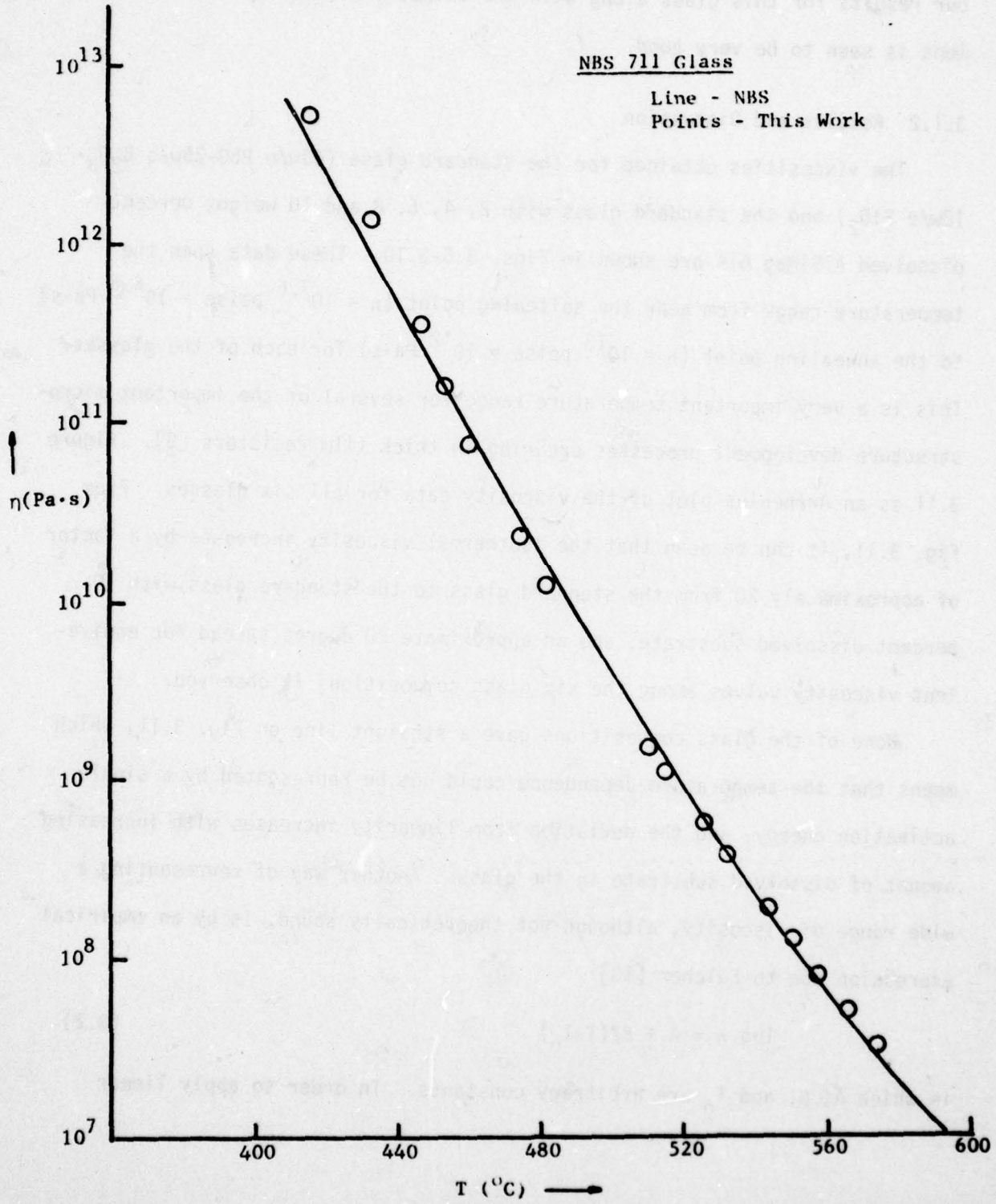

Figure 3.4. Viscosity of National Bureau of Standards No. 711.

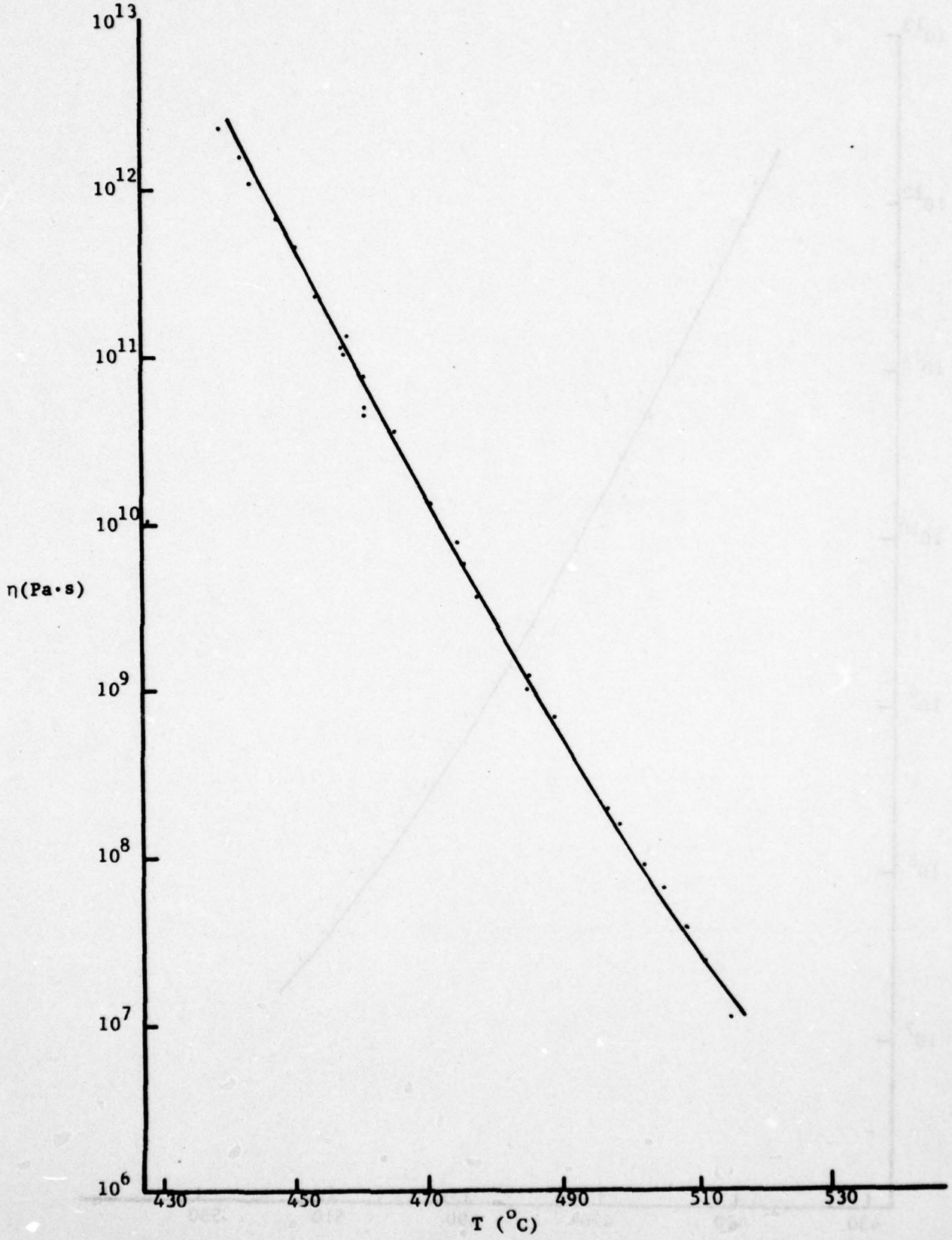

Figure 3.5. Viscosity of Standard Lead Borosilicate Glass.

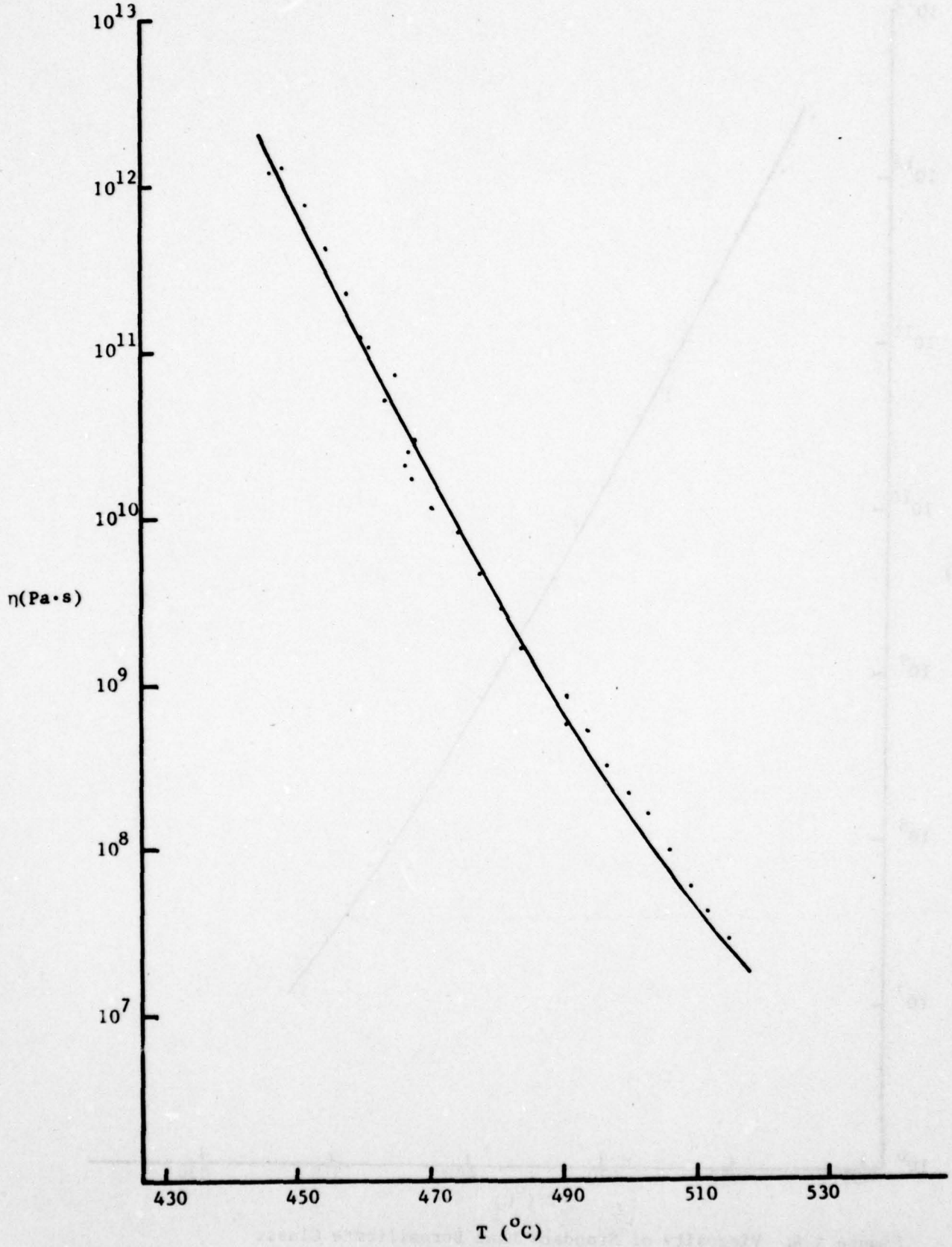

Figure 3.6. Viscosity of Standard Glass Containing 2 w/o Dissolved Substrate.

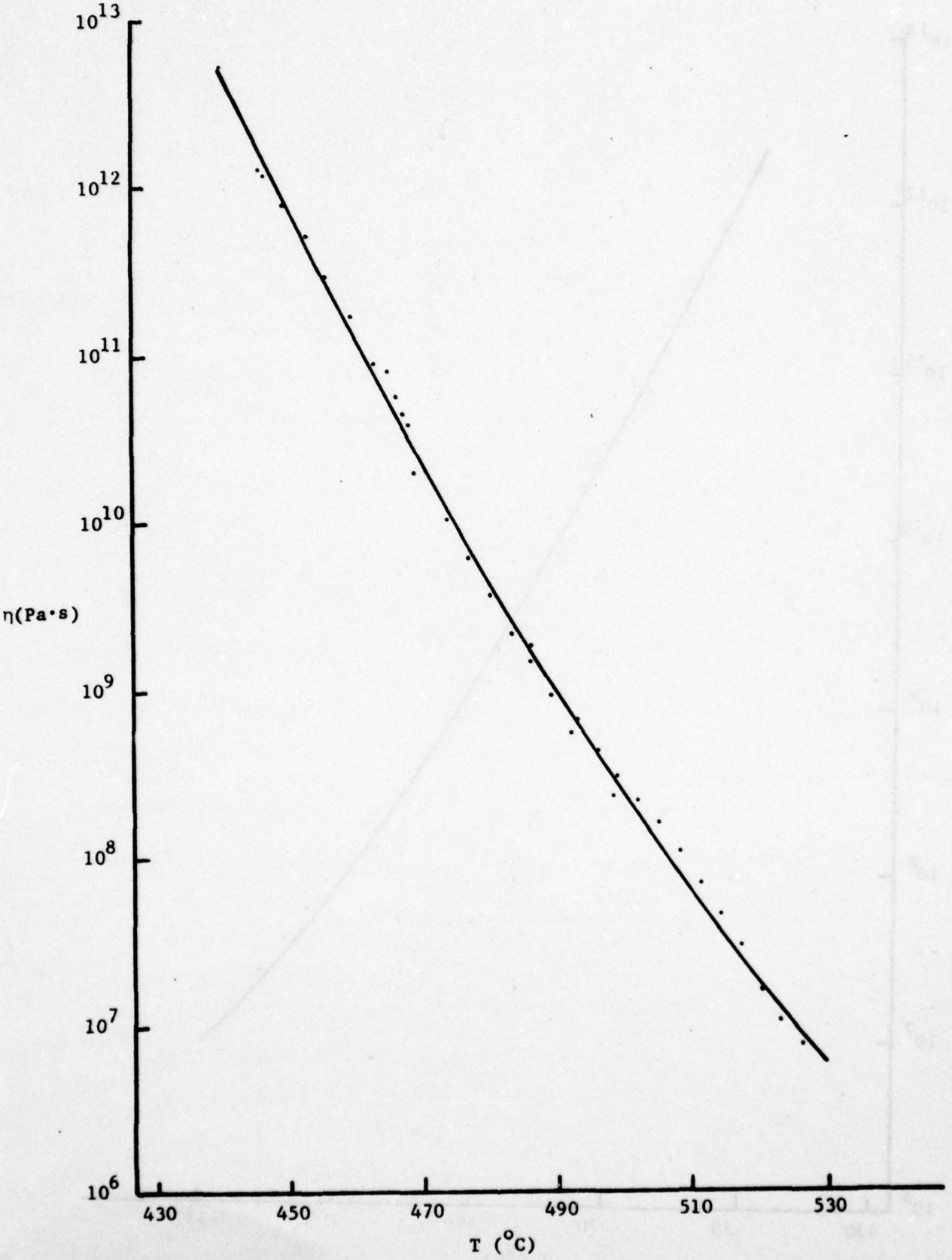

Figure 3.7. Viscosity of Standard Glass Containing 4 w/o Dissolved Substrate.

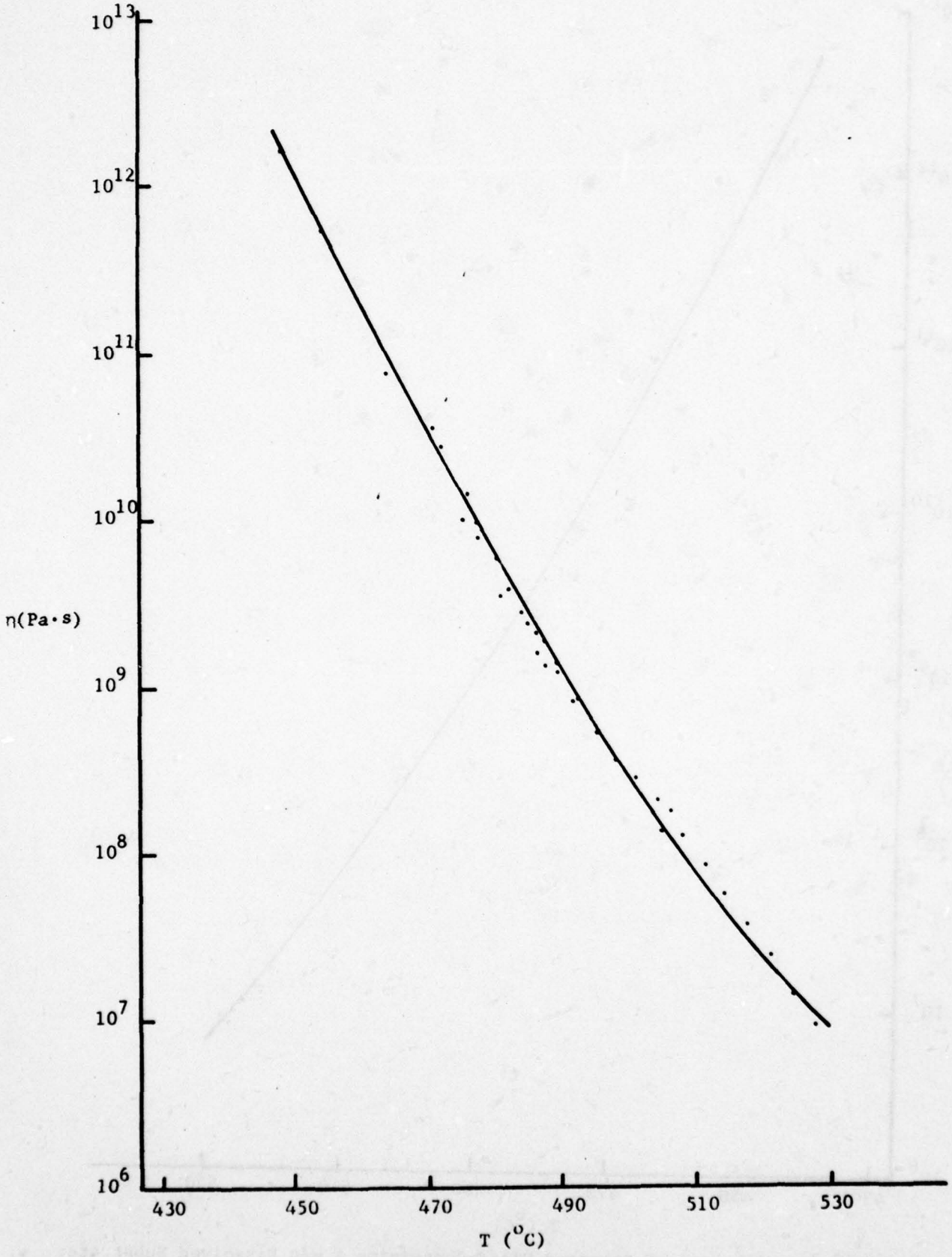

Figure 3.8. Viscosity of Standard Glass Containing 6 w/o Dissolved Substrate.

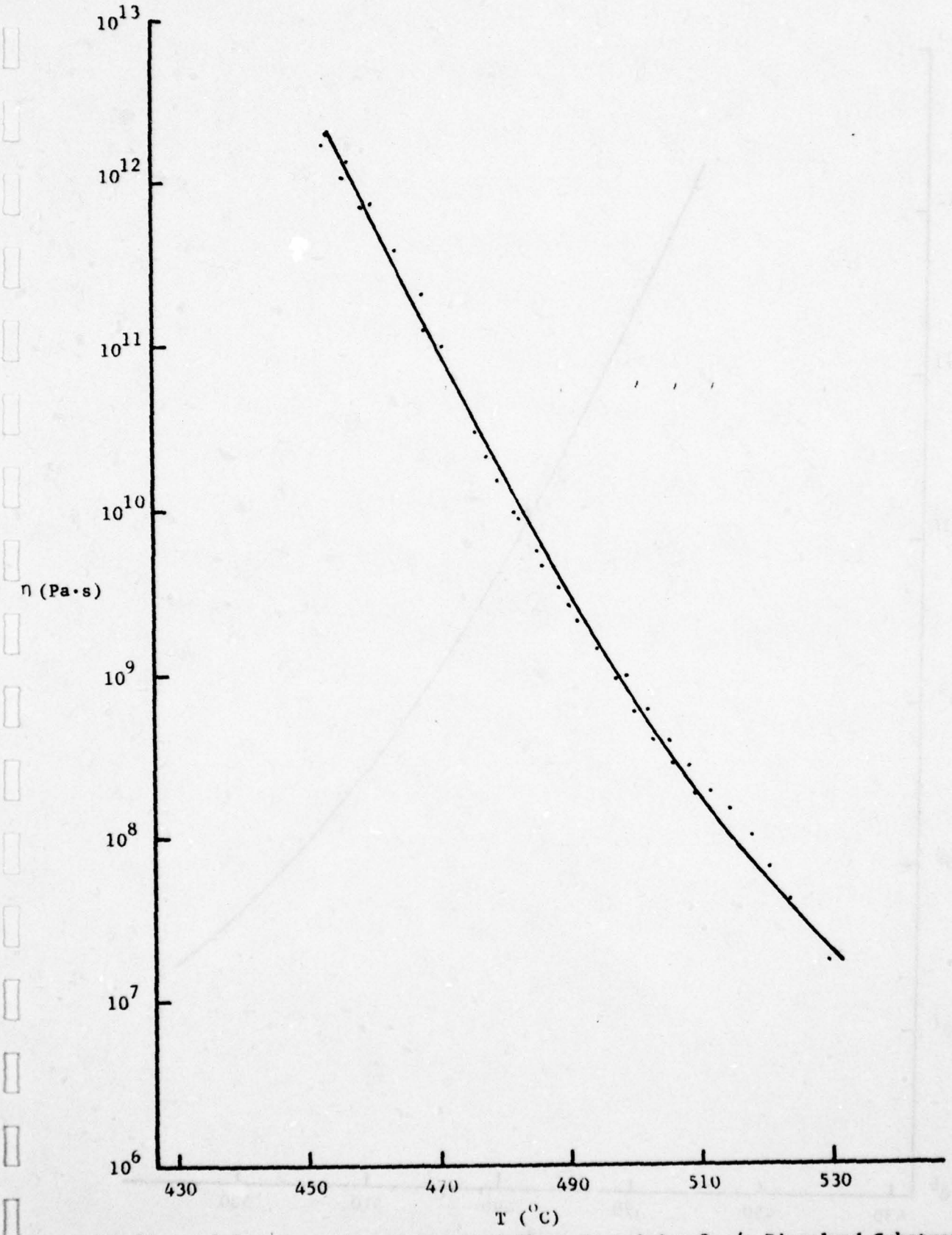

Figure 3.9. Viscosity of Standard Glass Containing 8 w/o Dissolved Substrate.

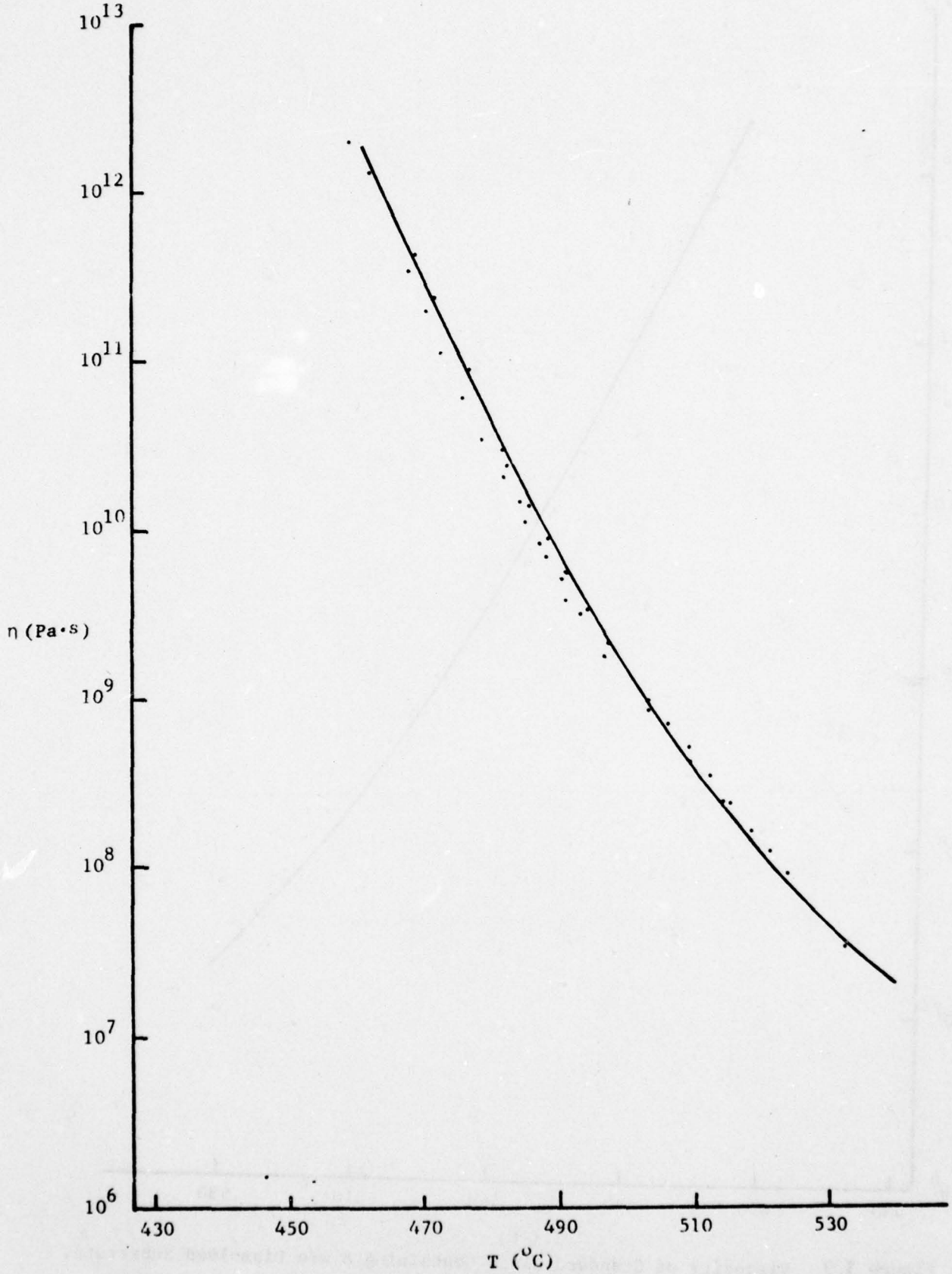

Figure 3.10. Viscosity of Standard Glass Containing 10 w/o Dissolved Substrate.

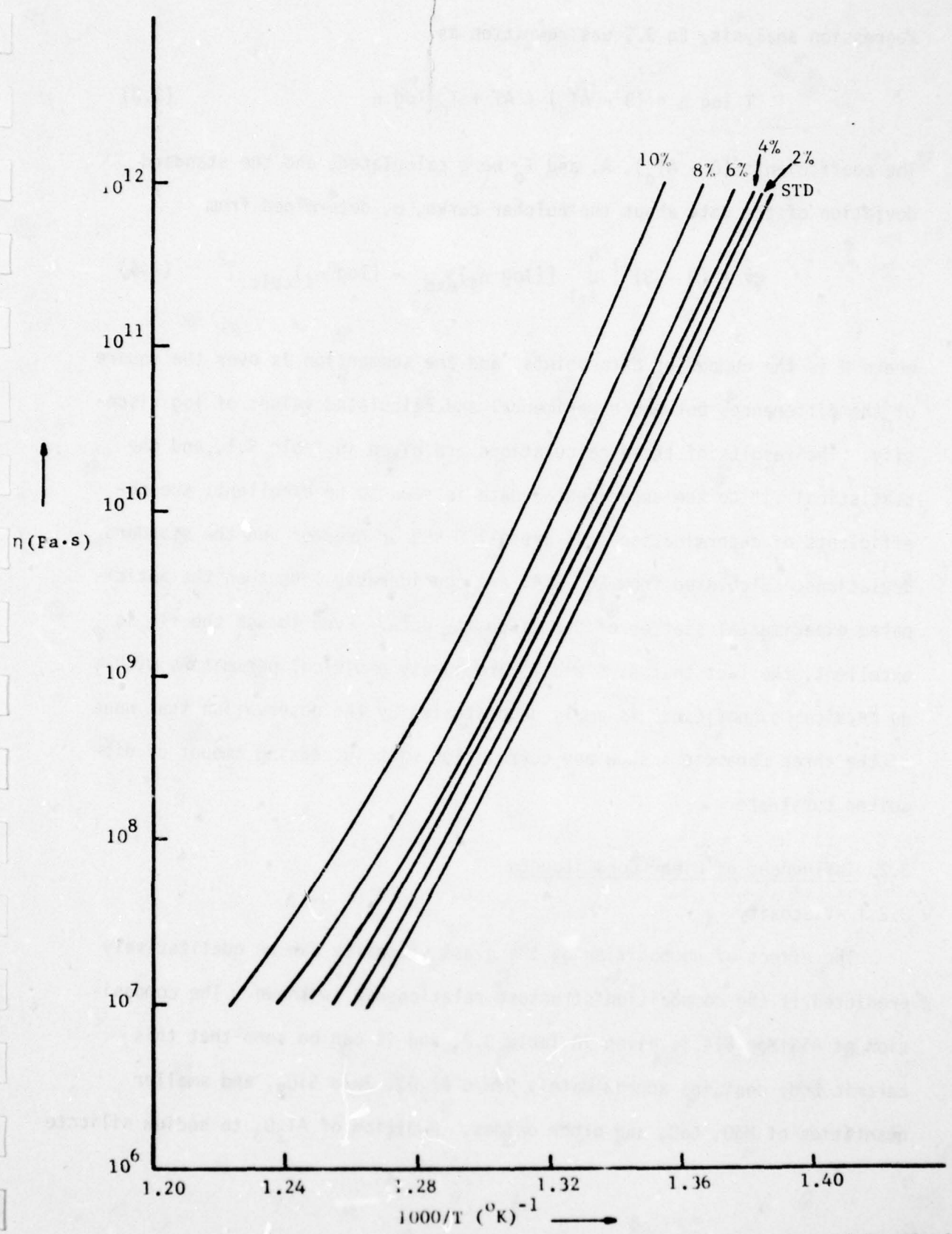

Figure 3.11. The Effect of Dissolved Substrate on the Viscosity of Standard Glass.

regression analysis, Eq 3.2 was rewritten as

$$T \log \eta = (B - AT_o) + AT + T_o \log \eta \qquad (3.3)$$

The coefficients $(B - AT_o)$, A, and T_o were calculated, and the standard deviation of the data about the Fulcher curve, σ, determined from

$$\sigma^2 = (N - 3)^{-1} \sum_{i=1}^{N} [(\log \eta_i)_{exp.} - (\log \eta_i)_{calc.}]^2 \qquad (3.4)$$

where N is the number of data points, and the summartion is over the square of the differences between experimental and calculated values of log viscosity. The results of these calculations are given in Table 3.1, and the statistical fit to the experimental data is seen to be excellent; the coefficients of determination (r^2) are all 0.999 or greater and the standard deviations, calculated from Eq. 3.4, are considerably less than the anticipated experimental scatter of the viscosity data. Even though the fit is excellent, the fact that A, B and T_o are purely empirical parameters with no physical significance is amply demonstrated by the observation that none of the three parameters show any correlation with increasing amount of dissolved substrate.

3.2 Influences of Minor Constituents

3.2.1 Viscosity

The effect of composition on the glass viscosity can be qualitatively predicted if the composition-structure relationship is known. The composition of AlSiMag 614 is given in Table 3.2, and it can be seen that this ceramic body contains approximately 96w/o Al_2O_3, 3w/o SiO_2, and smaller quantities of MgO, CaO, and other oxides. Addition of Al_2O_3 to sodium silicate

TABLE 3.1

FULCHER EQUATION FIT FOR EXPERIMENTAL GLASSES

Glass Composition	r^2	σ	A	B	T_o
Std. (63w/o PbO-25w/o B_2O_3-12w/o SiO_2	.9988	.0576	-2.11486	1916.50	585.02
Std. + 2w/o AlSiMag 614	.9994	.0389	-1.59694	1793.72	590.56
Std. + 4w/o AlSiMag 614	.9992	.0456	-4.19376	2794.29	549.85
Std. + 6w/o AlSiMag 614	.9995	.0323	-0.07368	1284.22	621.95
Std. + 8w/o AlSiMag 614	.9996	.0313	-0.42431	1475.82	612.77
Std. + 10w/o AlSiMag 614	.9997	.0225	1.60434	947.40	647.25

TABLE 3.2

COMPOSITION OF AlSiMag 614 CERAMIC

Constituent	Weight Percent	
	Typical[1]	Analyzed[2]
Al_2O_3	96.0	94.7
SiO_2	2.8	3.6
MgO	0.82	1.31
CaO	0.17	0.1
Fe_2O_3	0.09	0.2
Na_2O	0.06	0.001
K_2O	0.03	0.008
TiO_2	0.03	0.02
BaO	--	0.008
Cr_2O_3	--	0.003
Ga_2O_3	--	0.03
Mn_2O_3	--	0.001
ZrO_2	--	0.003

(1) A Typical Analysis according to the manufacturer, 3M Company of St. Paul, Minnesota.

(2) Bulk chemical analyses of the same lot of ceramic at RCA Laboratories, Princeton, New Jersey.

glasses [14] and lead silicate glasses [15] is known to increase the viscosity. Alumina, being an intermediate glass former, can enhance the network structure by increasing the bridging to nonbridging oxygen ratio. The low temperature viscosities measured by the beam bending method are consistant with these predictions. Silica, being a network former, is also expected to increase the viscosity. The effect of other oxides should be small because addition of even 10w/o substrate will introduce only about 0.1w/o of the other oxides into the glass.

The viscosity data for two glass compositions with 8w/o Al_2O_3 and 8w/o AlSiMag 614 substrate dissolved in the standard glass are given in Fig. 3.12. The minor constituents seem to have a greater influence than Al_2O_3 on the viscosity, but the difference is only $\pm$ 3°C in temperature for any given viscosity.

3.2.2 Surface Tension

There are only two compositions in the lead borosilicate system for which surface tension data are available [16], and calculation of surface tension using additivity factors is impractical due to nonlinearity caused by surface segregations. Therefore, the effect of the minor substrate constituents on surface tension was evaluated by combining viscosity data for the standard glass with varying amounts of dissolved AlSiMag 614 presented in Section 3.1.2 and the viscosity data for the standard glass with 8% dissolved alumina shown in Fig. 3.12 with data on surface tension to viscosity ratio calculated from initial stage sintering studies [7]. Due to the large temperature coefficient of viscosity ($\simeq$ 0.7 Pa·s/°C in the sintering range) of the glasses, the accuracy of this method is not high because even a small error in the temperature can cause an appreciable error in the calculated

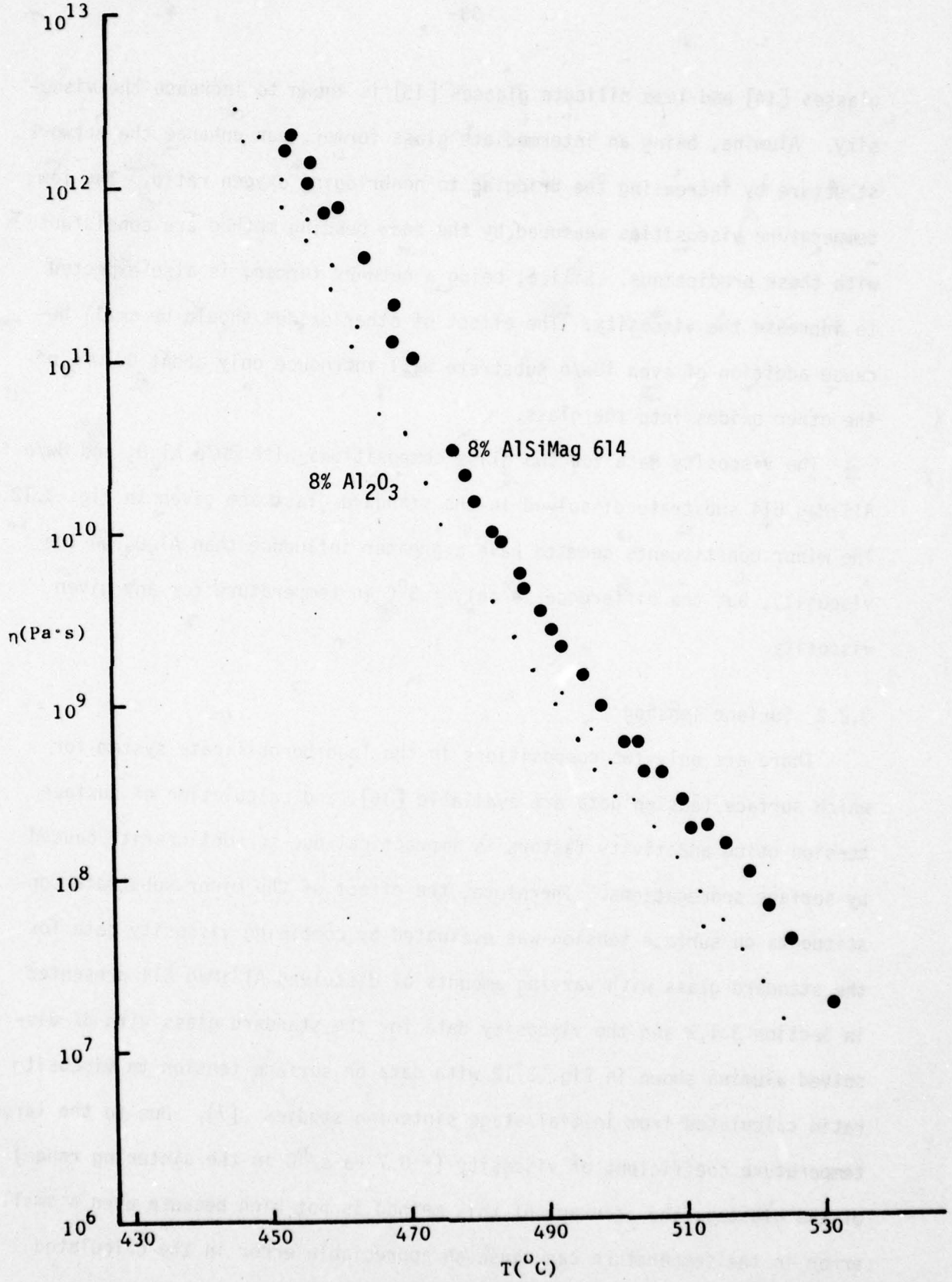

Figure 3.12. Comparison of Viscosities of Glasses with 8% Al_2O_3 and with 8% AlSiMag 614 Dissolved in Standard 63-25-12 Glass.

values of the surface tension. The surface tension values were calculated for all the experimental γ/η data using viscosity calculated from Fulcher fits to the viscosity data (Table 3.1). Assuming that the surface tension is constant in the sintering range, an average γ was calculated for each glass composition. Using the average γ, η values were calculated from the γ/η ratio and superimposed on the Fulcher lines. The average γ values and the superposition of calculated η on the Fulcher lines are shown in Fig. 3.13. The surface tension does not show any systematic variation with composition, and the differences may be due to uncertainties in the experimental data.

3.3 RuO_2 Solubility Studies

In order to develop an adequate model for the influence of the substrate on microstructure development and electrical properties of thick film resistors, it is necessary to know the influence of dissolved substrate on conductive ripening and sintering. Sintering and ripening of the conductive phase (RuO_2) are the two final processes in microstructure development of thick film resistors. In the initial stages of the sintering process, necks develop between adjacent RuO_2 conductive particles; as the sintering process proceeds, the necks grow until the adjacent particles coalesce to form larger particles. In the ripening process, the smaller particles preferentially dissolve and the material is transported through the liquid phase to precipitate on larger particles. The primary driving force for both sintering and ripening processes is the reduction in interfacial area between the conductive phase and the glass phase.

Earlier studies [3] have shown that the rate limiting step for the ripening of RuO_2 in 63-25-12 glass is the phase boundary reaction, that is,

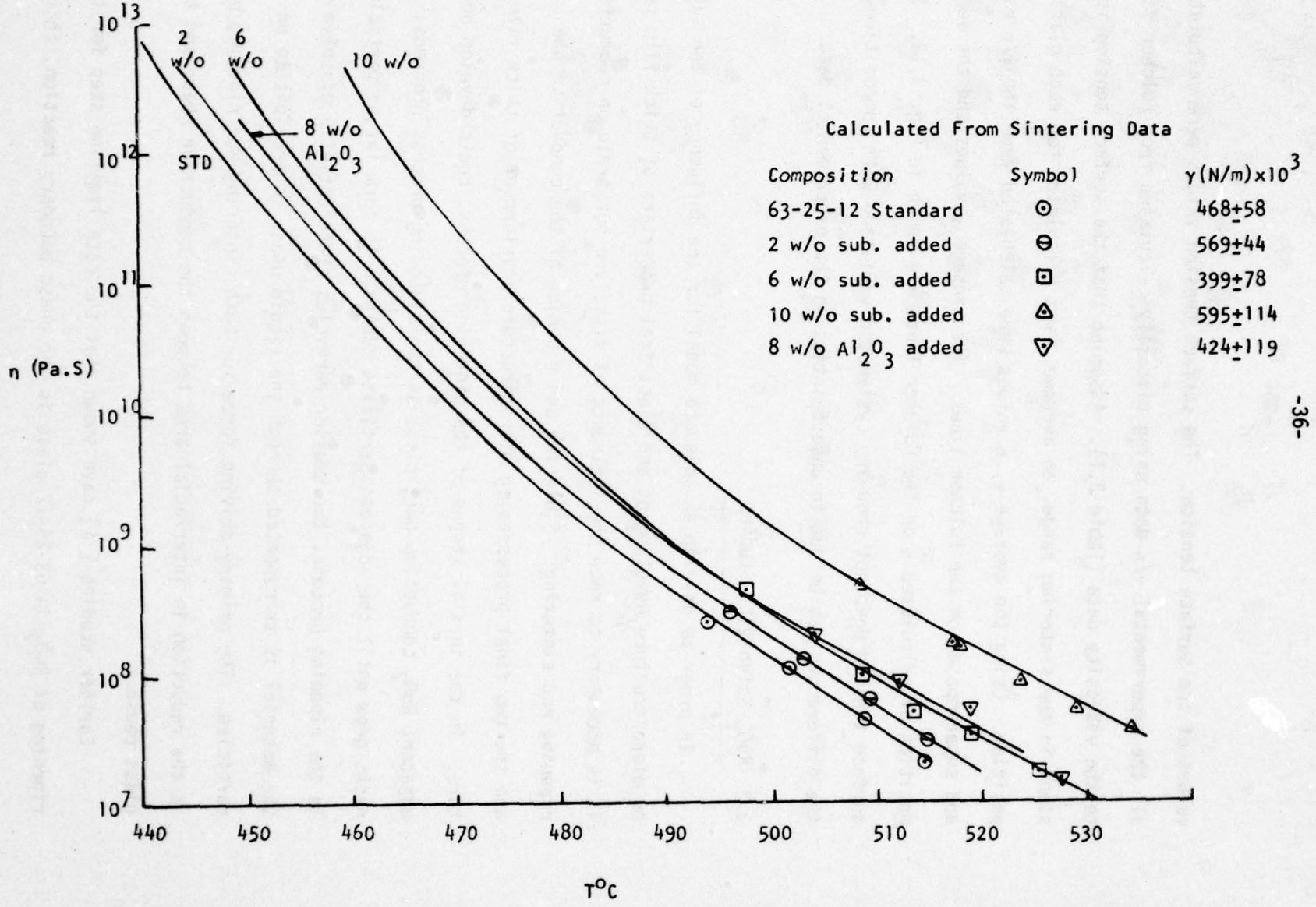

Figure 3.13. Comparison of Measured Viscosities (solid lines) with Viscosities Calculated from Sintering Data.

the rate of dissolution at the surface of the smaller particles or the rate of precipitation at the surface of the larger particles. If the kinetics of the initial stage sintering are also governed by the phase boundary reaction rate, then the relative neck growth between adjacent spherical particles will be given by [17]:

$$(x/r)^4 = (8\ k_1\ C_o\ \gamma_{sl}\ V_o\ K_T/k_2\ RT)r^{-2}\ t \qquad (3.5)$$

where

x = radius of the neck between adjacent particles at time t

r = radius of particles

C_o = equilibrium solubility of RuO_2 in glass

γ_{sl} = RuO_2-glass interfacial energy

V_o = molar volume

K_T = transfer coefficient

R, k_1 and k_2 = constants

It was also observed in the earlier ripening studies [5] that the presence of AlSiMag 614 substrate dissolved in the resistor glass decreased the rate of RuO_2 ripening. The decreased ripening kinetics could be due to a decrease in C_o, γ_{sl} or K_T, and the solubility studies were undertaken in order to determine the dependence of C_o on amount of dissolved substrate.

The experimental procedure which has been developed to determine the equilibrium solubility of RuO_2 in glass is as follows:

1. Prepare a powder mixture containing 10w/o RuO_2 and 90w/o glass containing varying amounts of dissolved AlSiMag 614 substrate.

2. Hold the RuO_2-glass mixture at the firing temperature (700, 800, 900, and 1000°C) in a platinum crucible for approximately 12 hours.
3. Quench the crucible in deionized water to minimize the possibility of reprecipitation of RuO_2.
4. Decompose the mixture using concentrated HCl with ultrasonic agitation.
5. Filter to remove the residue consisting of SiO_2, $PbCl_2$ and undissolved RuO_2.
6. Reduce the volume of the solution to an appropriate amount and determine the concentration of ruthenium in the solution with a Perkin-Elmer 303 Atomic Absorption Spectrophotometer which has been calibrated using standard $RuCl_3$ solutions.

The results of these experiments are given in Fig. 3.14 which shows the solubility of RuO_2 in the resistor glass as a function of amount of dissolved substrate at four different temperatures. The data shown in Fig. 3.14 are consistent with the magnitude of the solubility reported for RuO_2 in soda-silicate glasses [18, 19], and in the 63-25-12 lead borosilicate glass [1]. According to the results shown in Fig. 3.14, the solubility of RuO_2 in the standard 63-25-12 glass at 800°C is 9 ppm, which compares favorably with the result of 10 ppm obtained for the same conditions in the earlier work [1]. The solubility is seen to increase with increasing temperature and decrease with increasing amount of dissolved substrate, but the effect of dissolved substrate is highly nonlinear. The solubility decreases very sharply to nearly half of the original value with an addition of two percent substrate, but further additions of substrate have only a very slight effect on the RuO_2 solubility.

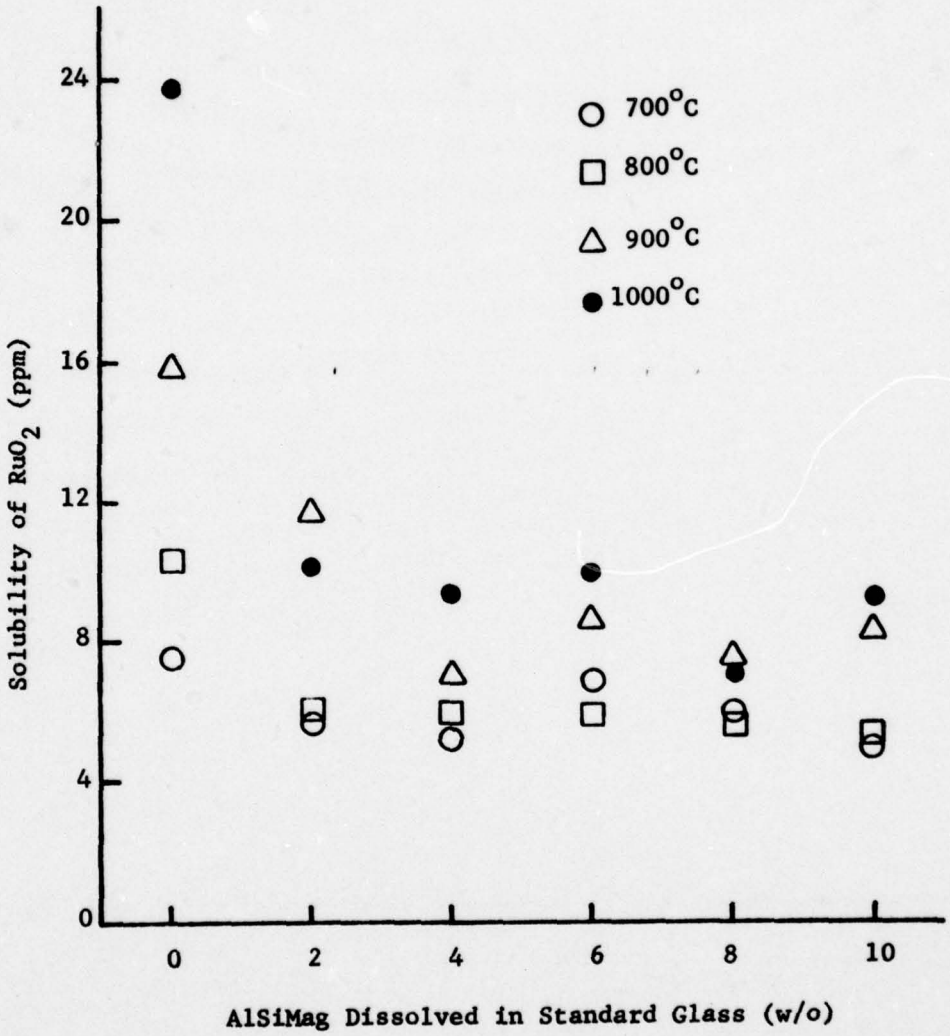

Figure 3.14. Influence of Dissolved Substrate on Solubility of RuO_2 in Standard (63 w/o PbO - 25 w/o B_2O_3 - 12 w/o SiO_2) Glass.

4. ELECTRICAL EFFECTS

4.1 Resistor Studies

4.1.1 Experimental

The standard 63-25-12 glass and three substrate glasses, 4, 6, and 10w/o substrate made by dissolving the appropriate amount of AlSiMag 614 substrate in the standard glass, were melted and fritted in deionized water. Following glass fabrication, the composition of the standard glass preparation was checked by chemical analysis following the procedures previously described [6]. Table 4.1 summarizes the important properties and compositions of the four glasses including annealing point, softening point, linear coefficient of thermal expansion, and density of each.

The glasses used in thick film inks are typically less than 50 μm in diameter with a whole spectrum of individual particle sizes. It has been postulated [5] and shown experimentally [20] that the particle size of the glass can greatly affect the electrical properties. Since we are interested in changes due to glass composition and not particle size, the glass used in this work was standardized to 13 μm or less by a sedimentation separation technique. The fritted glasses were crushed in a vibratory agate ball mill until they would pass through a 325 mesh (47 μm) screen. Then small quantities of glass were suspended in water, allowed to stand for a sufficient amount of time to let those particles > 13 μm to settle out, and the liquid containing the remaining particles was decanted off. Upon observation under a microscope, most particles collected were from 5 to 13 μm. It was not deemed necessary to separate the glass at a lower limit because the weight percent of glass particles less than 5 μm was quite small.

TABLE 4.1 COMPOSITION AND PROPERTIES OF GLASSES

	Composition by weight	Coefficient of expansion ($^oC^{-1}$) 25-300 ^oC	Density (kg/m^3)	Softening Point (^oC)	Annealing Point (^oC)
STD Glass	$63PbO-25B_2O_3-12SiO_2$	7.10×10^{-6}	4.55×10^3	522	445
4w/o Substrate	$60.5PbO-24.0B_2O_3-11.65SiO_2-3.85Al_2O_3$	6.80×10^{-6}	4.33×10^3	529	447
6w/o Substrate	$59.2PbO-23.5B_2O_3-11.5SiO_2-5.80Al_2O_3$		4.275×10^3	530	451
10w/o Substrate	$56.7PbO-22.5B_2O_3-11.2SiO_2-9.6Al_2O_3$		4.10×10^3	545	460

One of the most critical steps in the fabrication of thick film resistors is the blending of the inks. Insufficient blending can cause variations in conductor concentration from one resistor to the next, which in turn will lead to considerable scatter in electrical properties. This is especially significant for high value resistors where resistivity can change by orders of magnitude for a few percent change in conductive concentration relative to glass. However, too much blending will increase the chance of contaminating the ink with undesirable impurities (such as iron from the mixing rollers), and the particle size of the glass will decrease as blending time increases. To insure that observed differences in electrical behavior for resistors with different glass compositions was due to the amount of substrate dissolved and not to differences in blending, it was necessary to standardize the blending procedure. The four resistor pastes prepared for this work all contained 5w/o RuO_2 powder to 95w/o glass powder, the glasses being the standard 63-25-12, and the substrate glasses containing 4, 6, and 10w/o AlSiMag 614 substrate dissolved in the standard glass. The glass and RuO_2 dry powders were mixed by hand until a uniform gray color was achieved. The pastes were made by blending 40v/o of the mixed powders with 60v/o screening agent consisting of a solution of 10w/o N-300 ethyl cellulose binder in 90w/o butyl carbitol (diethylene glycol monobutyl ether) solvent. Initial blending was done by hand in the mortar before transfering to a motor driven stainless steel roller mill. The spacing between rollers and roller speed were kept constant during blending, and the inks were left on the mill until the standard deviation in the sheet resistance of test resistors gave reasonably low values. Table 4.2 summarizes the sheet resistance as a function of blending time on the roller mill for each resistor paste. When the standard deviation dropped below 5%,

TABLE 4.2

SHEET RESISTANCE AS A FUNCTION OF BLENDING TIME

	Standard Glass			4w/o Substrate Glass			6w/o Substrate Glass			10w/o Substrate Glass		
Hours Blended	R_s (kΩ)	σ (kΩ)	%σ	R_s (kΩ)	σ (kΩ)	%σ	R_s (MΩ)	σ (MΩ)	%σ	R_s (MΩ)	σ (MΩ)	%σ
0.0	222	21	10%	937	87	9%	2.5	1	40%	>300		
0.5												
1.0	147	13	9%	589	63	10%				31.7	23	73%
1.5							.447	.011	2.5%			
2.0	129	10	8%	542	53	10%				4.00	.012	.3%
2.5												
3.0	104	10	10%	550	30	5.5%						
3.5				436	20	4.5%						
4.0	90.7	2	2%									

blending was terminated. It is interesting to note that as the weight percent of substrate increases, the blending time required for good mixing decreases. This could be due to the decreasing glass density for increasing weight percent substrate.

Several conductive pastes were considered for use as electrodes with the resistive inks. Five commercial and one in-house conductive (platinum powder with the standard 63-25-12 glass as a binder) were evaluated. The conductives were screened and fired onto AlSiMag 614 substrates following procedures recommended by the manufacturers. The resistance of the conductive runs were measured, and relative values are given in Table 4.3. In addition, resistors with 5w/o RuO_2 and 95w/o standard glass were fired in batches at 930°C for 10 minutes or in a belt furnace using a typical firing profile. Sheet resistance was measured and visual observations made with a stereo microscope of the resistor/conductor interface. Comparison of the sheet resistance values for the resistors fired over different conductive inks shows quite dramatically the importance of selecting the proper conductor. Using the same firing schedule, the sheet resistance varied from 55 kΩ to 640 kΩ, and this wide deviation can be attributed solely to the resistor/conductor interface. Under visual observation, the high value resistors showed a decreased density of the RuO_2 resistor networks near the resistor/conductor interface. Based on these experiments, the DuPont 9885 platinum-gold conductive was chosen for the resistor experiments.

Resistors were screened in a rectangular pattern for each of the four formulations so that there was one square between the voltage electrodes. The printed resistors were dried at 130°C for 30 minutes followed by an additional 30 minutes at 300°C to insure complete removal of the organic binder. To

TABLE 4.3 CONDUCTIVE TERMINATION EXPERIMENTS

Conductor Number	Conductive Particles	Conductor Relative Resistance	R_s of Resistors Fired at 930°C, 10 min. (kΩ)	R_s of Resistors Fired in Belt Furnace (kΩ)	Interface Appearance
Du Pont 9308	Pd-Ag	0.50	182.15	171.63	Segregation
Du Pont 9755	Pt-Ag	0.85	165.57	188.05	Segregation
Du Pont 9770	Pt-Ag	0.25	637.5	207.77	Run-out of Res. onto Electrodes
Du Pont 9885	Pt-Au	1.10	62.9	110.64	No segregation, good mixing at interface
Engelhard A-3380	Pt	1.50	55.11	101.48	Segregation
STD Glass 10%	Pt	1.40	250	--	Segregation

prevent adsorption of moisture or other forms of contamination, resistors were stored in an evacuated desicator until high temperature firing. The dissolution experiments discussed in Section 2 were performed by rapidly bringing the samples to temperature, holding for an appropriate time, then rapidly cooling them to room temperature. In order to make use of the curves thus generated, a similar procedure was employed for resistor firing. Four resistors were placed on a ceramic tile (which was marked and used for all subsequent resistor firings) and heated to 130°C for 10 minutes to remove any moisture that might have been adsorbed since screening and drying. The resistors were then transferred to a box furnace for an appropriate time, then removed and air cooled to room temperature. Substrates were weighed before resistor printing and again after firing in order to determine the weight of the resistive film. The resistor length and width were measured using a calibrated stage on a stereo microscope, and employing the density of the appropriate glass from Table 4.1 (corrected to allow for 5w/o RuO_2) the resistor volume was calculated. Dividing by the length and width gave an average thickness of the film so that all sheet resistances could be normalized to a 25 μm thickness.

Two different firing experiments were conducted. In one, the firing time was held constant at 10 minutes while varying the temperature (650, 700, 725, 750, 800, 850, 900, or 950°C), while in the other the firing temperature was set at 800°C and the firing time was varied from 3 to 22 minutes. Four resistors of each glass composition were fired at each temperature or time, and data points that appear on all subsequent test results are averages of four samples.

The experiments included measuring sheet resistance, hot and cold TCR, resistance as a function of temperature, and noise index all as a function of the firing parameters. The resistance between the inner electrodes of the four-terminal configuration was determined by measuring the voltage drop across the inner terminals and the voltage drop across a precision standard resistor in series with the device under test. A simple calculation then gave the sample resistance, and the resistivity was calculated from the geometry measurements. An average resistor volume was calculated first by summing the resistor weight of all samples fired of a given glass composition then dividing by the number of samples and the density of the resistor glaze. It was assumed that the volume of glass between the inner electrodes remained constant, and since the resistor length did not vary during firing, the product of thickness and width, the cross sectional area, must also remain constant. A Dektak profilometer was used to measure the cross-sectional area of several resistors from different glasses firing conditions; even though the resistor width increased for increasing firing time and temperature, the thickness decreased in such a manner that the cross-sectional area did indeed remain constant. This makes it possible to directly relate changes in resistance with changes in resistivity.

The incremental form of the temperature coefficient of resistance (TCR) is defined as:

$$TCR = \frac{R_T - R_{RT}}{R_{RT}(T - RT)} \times 10^6 \ (ppm/^oC) \qquad (4.1)$$

where R_T is the sample resistance at temperature T, R_{RT} is the resistance at room temperature, and TCR is measured in parts per million per degree centigrade. The resistance of all samples was measured at room temperature and

125°C to calculate the hot TCR, followed by a measurement at -55°C to calculate the cold TCR. To facilitate the temperature cycling of a large number of samples, hot and cold temperature baths were assembled. The 125°C measurements were done in an oil bath heated on a hotplate equipped with a magnetic stirrer to maintain a constant temperature throughout the bath. Two chromel-alumel thermocouples were used, one as a sensor to a temperature controller and the second to measure the sample temperature. The bath temperature was found to be 125°C $\pm$ 2°C for long periods of time, and samples quickly stabilized (less than 10 seconds) when immersed in the oil. For the -55°C bath, an immersion cooler was placed in a dewar flask filled with trichloroethylene (TCE), which was found to be ideal as the cooling medium because it maintains a high impedance, unlike acetone or the alcohols. Resistors stabilized in less than 20 second after immersion, and the bath temperature, measured with a chromel-alumel thermocouple, was recorded along with the sample resistance. To initiate the sequence of measurements, each resistor was inserted into a special harness made with four quick disconnect leads, immersed in a beaker of TCE at room temperature and the resistance measured. The sample was then placed in the oil bath to record the 125°C resistance. The oil was removed with TCE, which also cooled samples to room temperature where resistance was measured again. The room temperature values were always found to be within 0.1% of the original value. The sample was then transferred to the cold temperature bath, where resistance and temperature were recorded before returning to room temperature. Initially this procedure was repeated three times for each sample, but no variation in resistance at any of the three test temperatures could be detected. Subsequently, resistors were only tested once at 125 and -55°C.

In addition to the measurement of hot and cold TCR, several devices were selected for a more complete resistance versus temperature profile. These resistors were mounted on a copper block to establish thermal equilibrium and placed in an environmental chamber capable of continuous temperature variation from -55 to +125^{o}C. The sample resistance and temperature (thermocouple emf) were plotted simultaneously on an X-Y recorder to facilitate the testing of a number of devices.

All resistors prepared for this work were tested for their noise characteristics by employing the Quantech noise test method [21]. The noise index (NI) in decibels (dB) over a decade of frequency is defined as follows:

$$NI = 20 \log \left(\sqrt{\overline{v^2}} / V \right) \tag{4.2}$$

where $\sqrt{\overline{v^2}}$ is the rms current noise voltage measured in microvolts and V is the dc applied voltage across the resistor measured in volts. Rearranging the equation in the following form

$$NI = 20 \log \sqrt{\overline{v^2}} - 20 \log V, \tag{4.3}$$

and identifying the terms on the right as the decibel equivalents of the current noise voltage and dc bias voltage, respectively, illustrates how the Quantech measurement is made. A dc bias is applied to the device under test and is measured by a dc voltmeter in dB while an ac band-pass amplifier measures the rms current noise voltage in microvolts and displays it in dB. The noise index is then calculated as the difference in the two readings. A calibration source is also used to calibrate the system to account for resistor loading. The Quantech system is strictly a two terminal measurement; therefore, the noise measured is not necessarily that of the resistor body

alone but will also represent any contributions from the resistor/conductor interface and noise of the lead wires.

4.1.2 Results and Discussion

The sheet resistance for all four resistor inks is plotted as a function of firing time in Fig. 4.1. The resistance decreases very rapidly with increasing firing time followed by a region of a fairly constant resistance for longer firing times. These results support the model for microstructure development presented in Section 1. The rapid decrease in resistance corresponds to the initial stages of micronetwork formation where the RuO_2 chains are forming by sintering of contacts. After a few minutes, the networks have developed to a point where no further significant growth can occur and resistance levels off. Additional changes are expected until conductive ripening begins when resistance will increase due to the growth of large RuO_2 particles at the expense of smaller particles. However, the kinetics of ripening are sufficiently slow that no signs of this process occurring are observed. The time required to develop a measurable resistance (10"Ω using a Keithley 602 Electrometer) and the time required to reach constant sheet resistance are both seen to increase with increasing amount of substrate dissolved in the resistor glass. This result is also consistent with the model which predicts reduced kinetics for the development of RuO_2 networks as the glass viscosity increases. In addition, it is noted that an increased amount of substrate dissolved in the glass increases the magnitude of the sheet resistance in the constant resistance region. This may indicate that the resistance of the non-sintered contacts as well as their relative number in the RuO_2 chains increases with increasing amount of substrate.

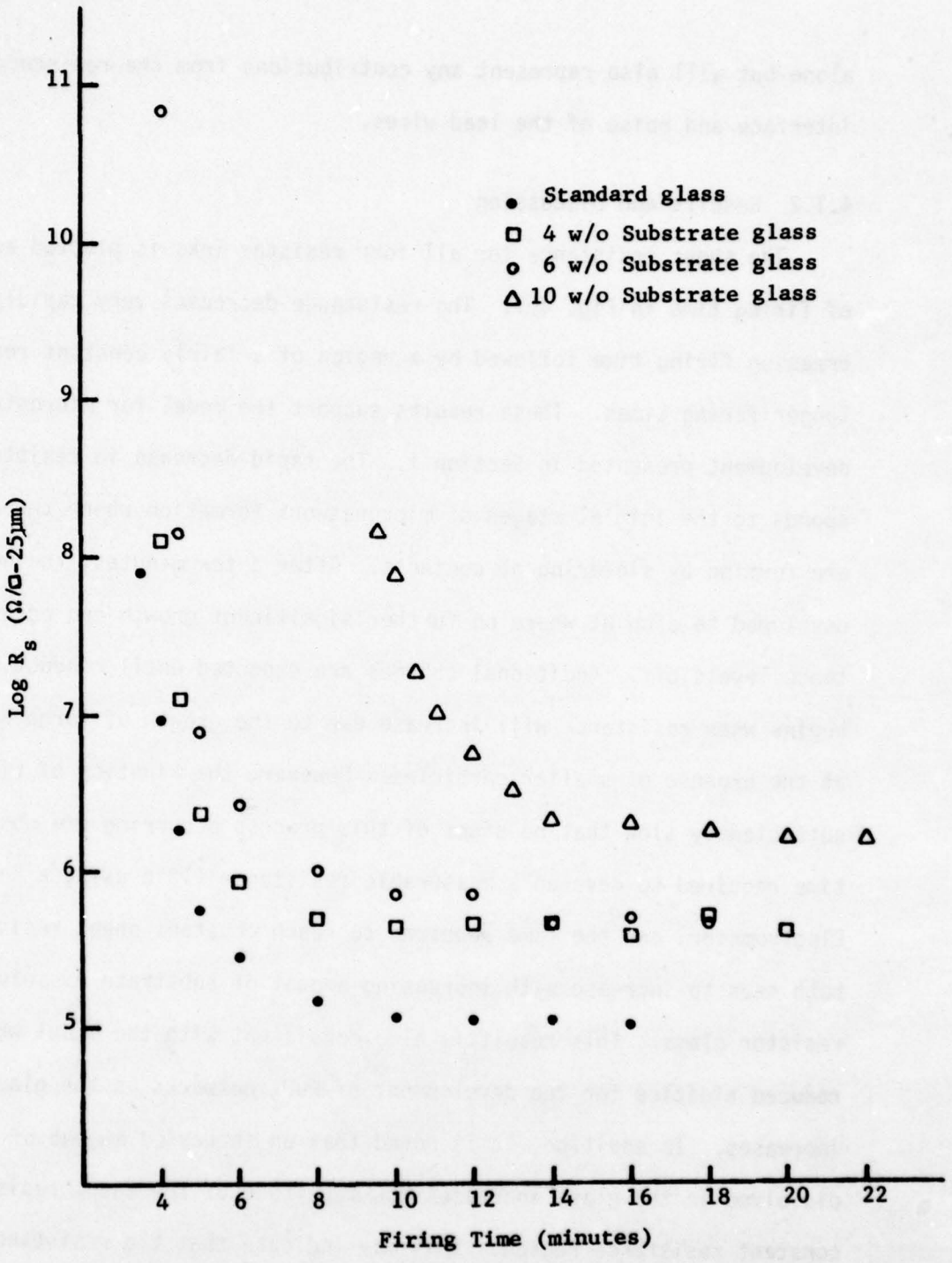

Figure 4.1. Sheet Resistance versus Firing Time at 800°C.

Similar conclusions can be drawn from the graph of sheet resistivity versus firing temperature in Fig. 4.2. The rapid decrease in resistance is observed followed by a region where resistance is fairly constant, although the latter is not as pronounced as in Fig. 4.1. This can be explained by the fact that the kinetics of microstructure development are exponentially dependent on temperature and only dependent on time to some power. Increasing the amount of substrate in the glass phase results in an increased temperature for measurable resistance; from standard glass to 10w/o substrate glass, there is about a 100^{o}C difference in firing temperature required to achieve the same sheet resistance. Based on the data for softening point and glass viscosity as a function of substrate concentration, one would expect to see such a shift.

One of the most powerful tools for investigating conduction mechanisms in any system is by temperature variation. By measuring the current as a function of applied voltage and temperature then correlating the data with the theory, strong arguments for specific mechanisms can often be formed. However, an interesting phenomenon in thick film resistors is the observation that they may have either a positive TCR, or negative TCR, or <u>both</u> in the vicinity of room temperature. The TCR's are typically quite low ($< \pm$ 300 ppm/^{o}C), a characteristic which makes them attractive for critical circuit applications. There are many factors that determine the temperature dependence a particular resistor will have, including glass composition and firing time-temperature.

The results of the hot TCR measurements are presented in Figs. 4.3 and 4.4. Figure 4.3 shows hot TCR as a function of firing time at 800^{o}C while Fig. 4.4 gives the hot TCR for samples fired for 10 minutes as a function of temperature. In both of these experiments, the hot TCR was found to increase

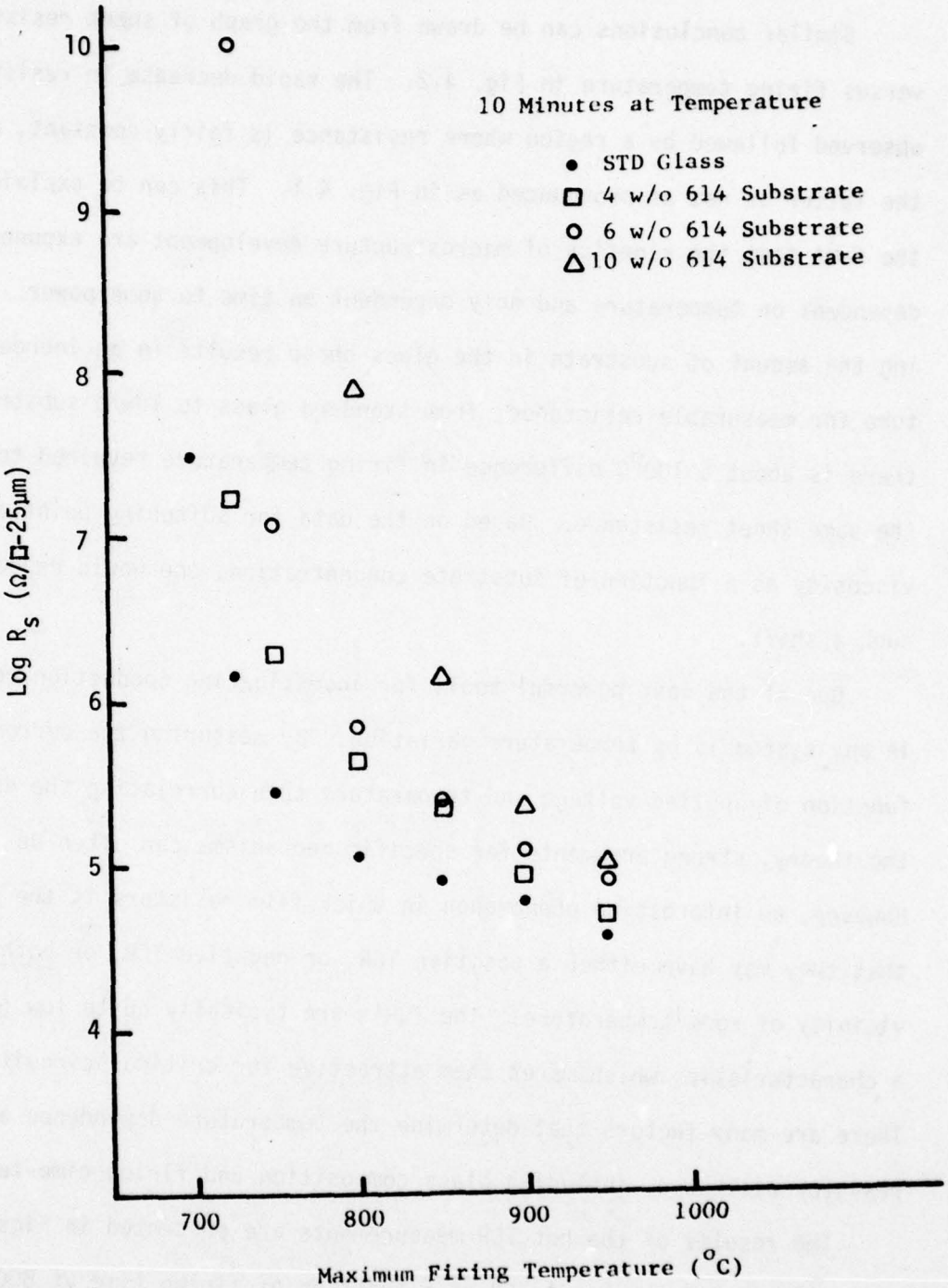

Figure 4.2. Sheet Resistance as a Function of Firing Temperature.

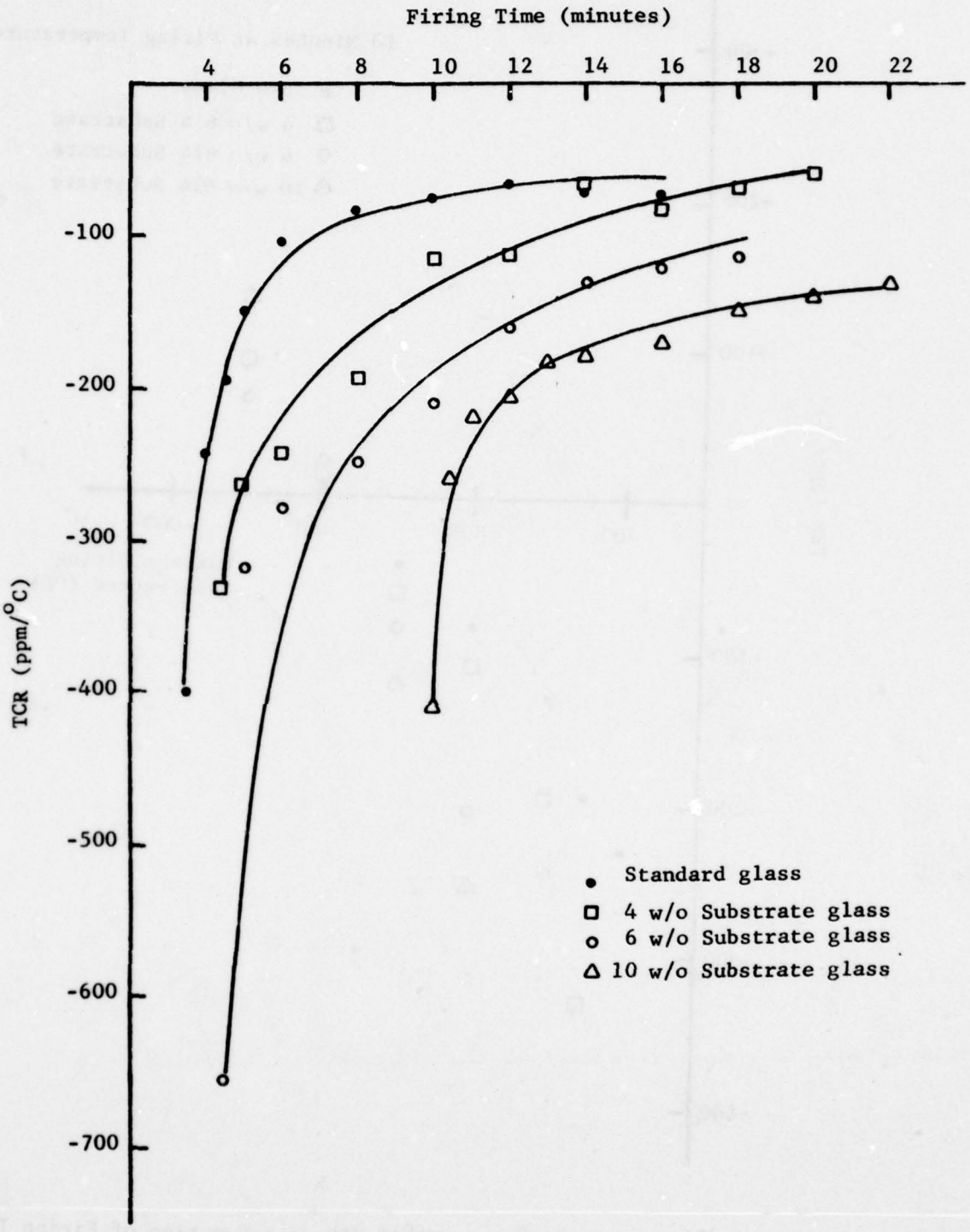

Figure 4.3. Hot (25° to 125°C) TCR versus Firing Time at 800°C.

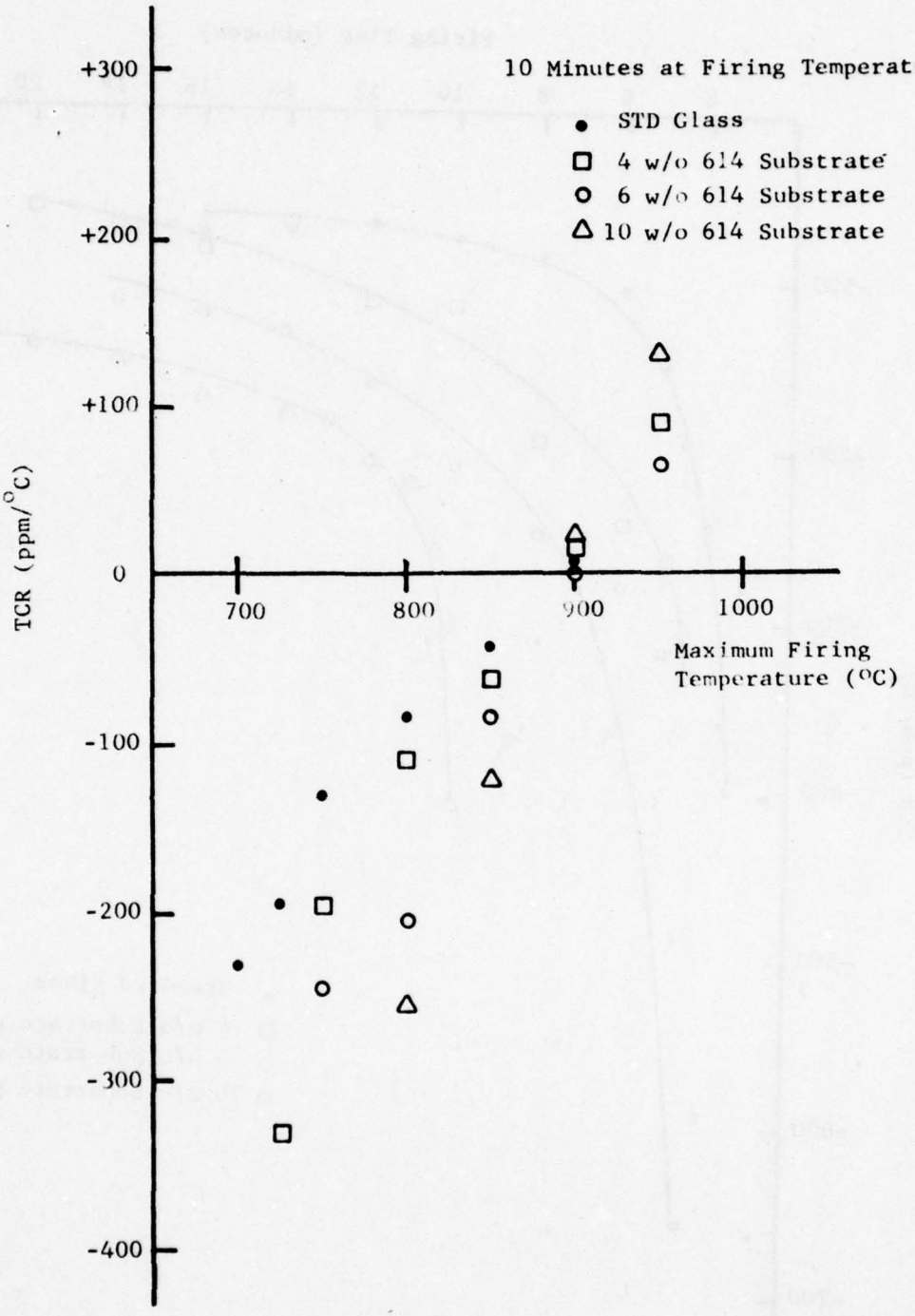

Figure 4.4. Hot (25°C to 125°C) TCR as a Function of Firing Temperature.

with increasing firing time or temperature for each glass composition. The increase is very rapid initially, as might be expected based on the rapidly changing sheet resistance of the samples (Figs. 4.1 and 4.2), but levels off for continued firing, indicating that very little change in microstructure is taking place. The microstructure development model predicts that during the early part of network formation, most chains contain large numbers of non-sintered contacts which are converted to sintered contacts as firing proceeds. The increasing values of TCR as a function of firing time/temperature support this argument because the temperature dependence of non-sintered contacts is negative while the sintered contacts exhibit positive TCR's. The hot TCR increases for decreasing weight percent substrate at all firing times (Fig. 4.3), and this is also the behavior observed for the hot TCR vs. firing temperature (Fib. 4.4) up to 850^{o}C. Above this temperature there is very little difference in TCR among the four glass compositions, and this is probably indicative of the fact that there is little difference in glass compositions at these temperatures due to the dissolution of the substrate during resistor firing. The sheet resistances of the different glasses are also very close at 900^{o}C and above (Fig. 4.2), implying that the characteristics of the separate glasses are beginning to converge.

The cold TCR as a function of firing time and firing temperature for resistors made from the four glass compositions are presented in Figs. 4.5 and 4.6 respectively. The results follow the same trends as the hot TCR data, but an interesting and important comparison between the two experiments can be made. At any given firing time or temperature, the cold TCR is more negative than the hot TCR. This conclusion is important because it is consistent with the model of non-sintered thermally activated contacts as being integral

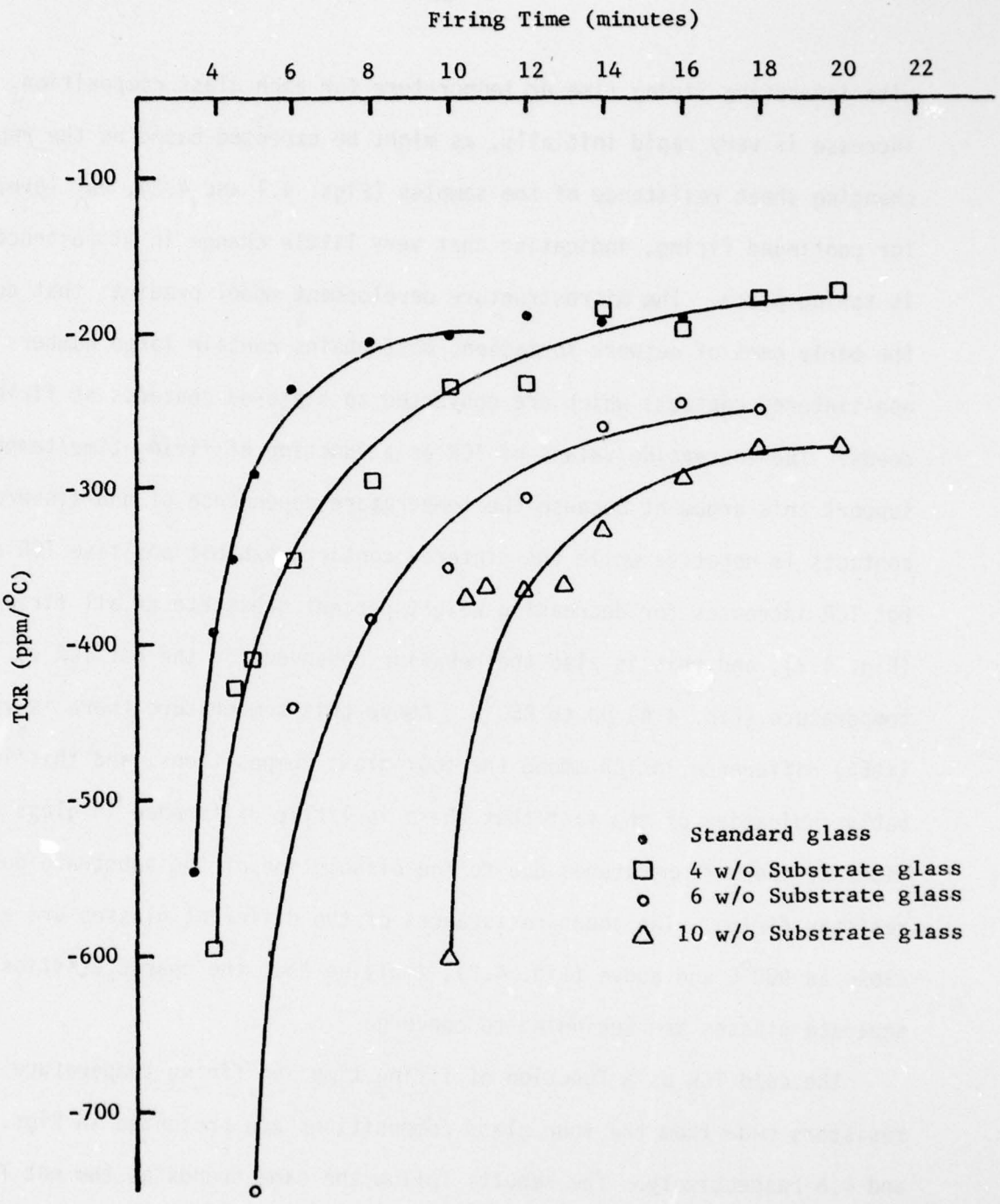

Figure 4.5. Cold (-55° to 25°C) TCR as a Function of Firing Time at 800°C.

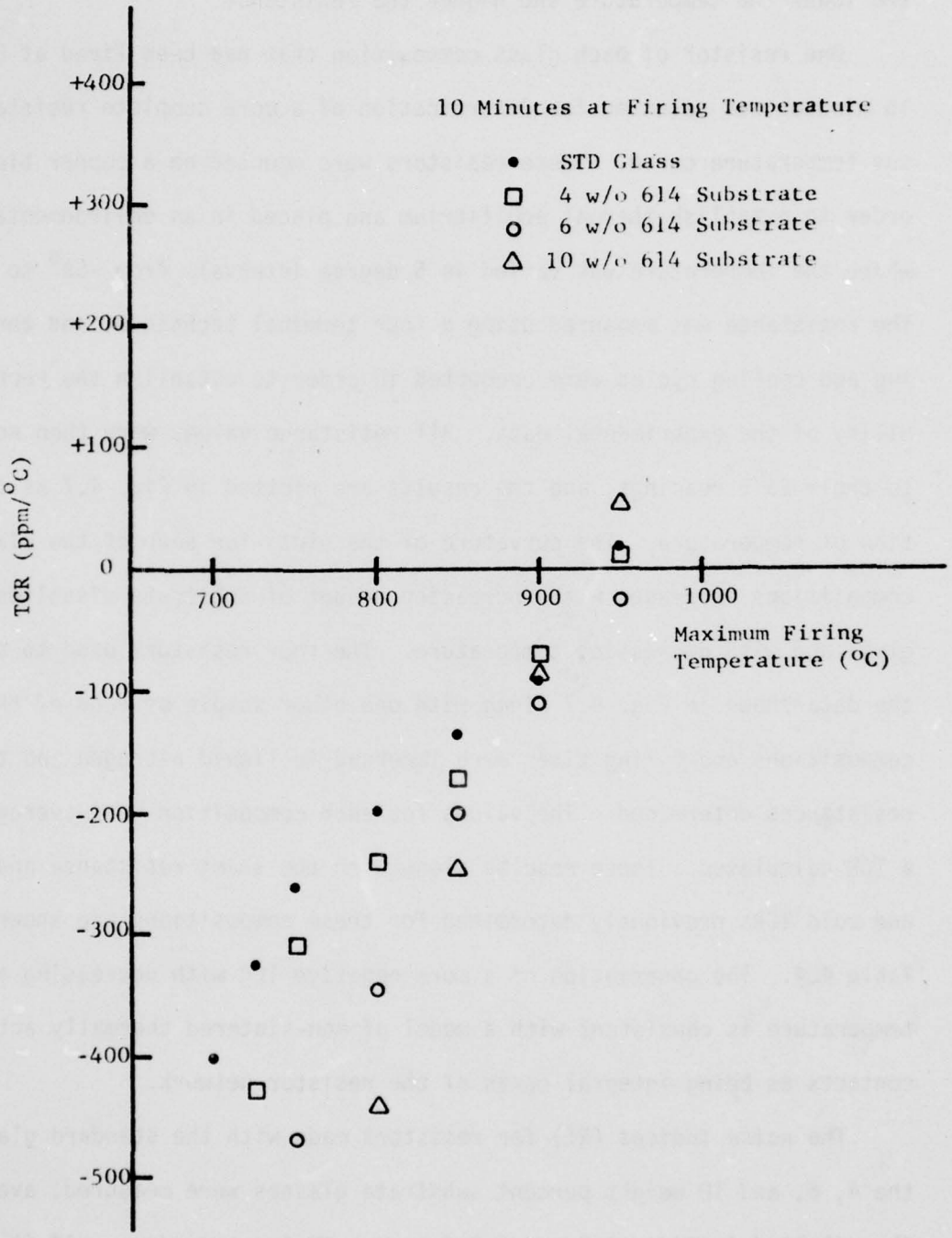

Figure 4.6. Cold (-55° to 25°C) TCR as a Function of Firing Temperature.

parts of the resistive networks. If there are thermally-activated contacts, the lower the temperature the higher the resistance.

One resistor of each glass composition that had been fired at 800°C for 16 minutes was selected for determination of a more complete resistance versus temperature curve. These resistors were mounted on a copper block in order to establish thermal equilibrium and placed in an environmental chamber where the temperature was varied in 5 degree intervals from -55° to 125°C. The resistance was measured using a four terminal technique, and three heating and cooling cycles were conducted in order to establish the reproducibility of the experimental data. All resistance values were then normalized to their 25°C readings, and the results are plotted in Fig. 4.7 as a function of temperature. The curvature of the plots for each of the glass compositions increases with increasing amount of substrate dissolved in the glass and with decreasing temperature. The four resistors used to obtain the data shown in Fig. 4.7 along with one other sample of each of the same compositions and firing times were immersed in liquid nitrogen and their resistances determined. The values for each composition were averaged and a TCR calculated. These results along with the sheet resistance and the hot and cold TCRs previously determined for these compositions are shown in Table 4.4. The observation of a more negative TCR with decreasing average temperature is consistant with a model of non-sintered thermally activated contacts as being integral parts of the resistor network.

The noise indices (NI) for resistors made with the standard glass and the 4, 6, and 10 weight percent substrate glasses were measured, averaged, then plotted in Figs. 4.8 and 4.9 for each firing procedure. If it is assumed that the primary contributor to noise is the non-sintered contacts in the

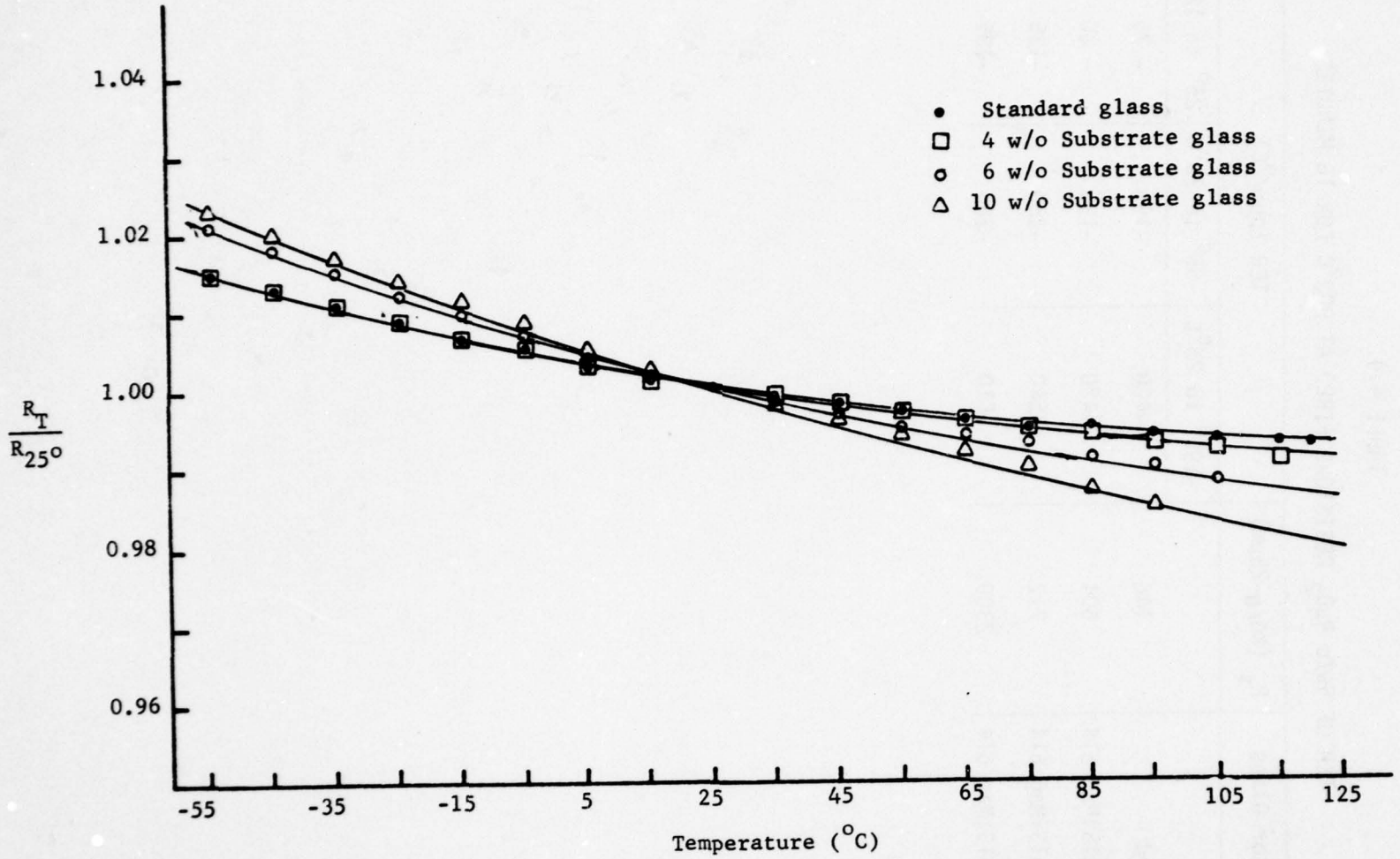

Figure 4.7. Temperature Dependence of Resistance for Resistors Fired at 800°C for 16 Minutes.

TABLE 4.4

TCR OF 5w/o RuO_2 RESISTORS FIRED AT 800°C FOR 16 MINUTES

Resistor Glass	R_s (kΩ/□-25μm)	TCR (ppm/°C)		
		-196° to 25°C	-55° to 25°C	25° to 125°C
Standard	146	-420	-190	- 75
4w/o AlSiMag 614	604	-420	-195	- 80
6w/o AlSiMag 614	717	-540	-250	-125
10w/o AlSiMag 614	2300	-510	-285	-195

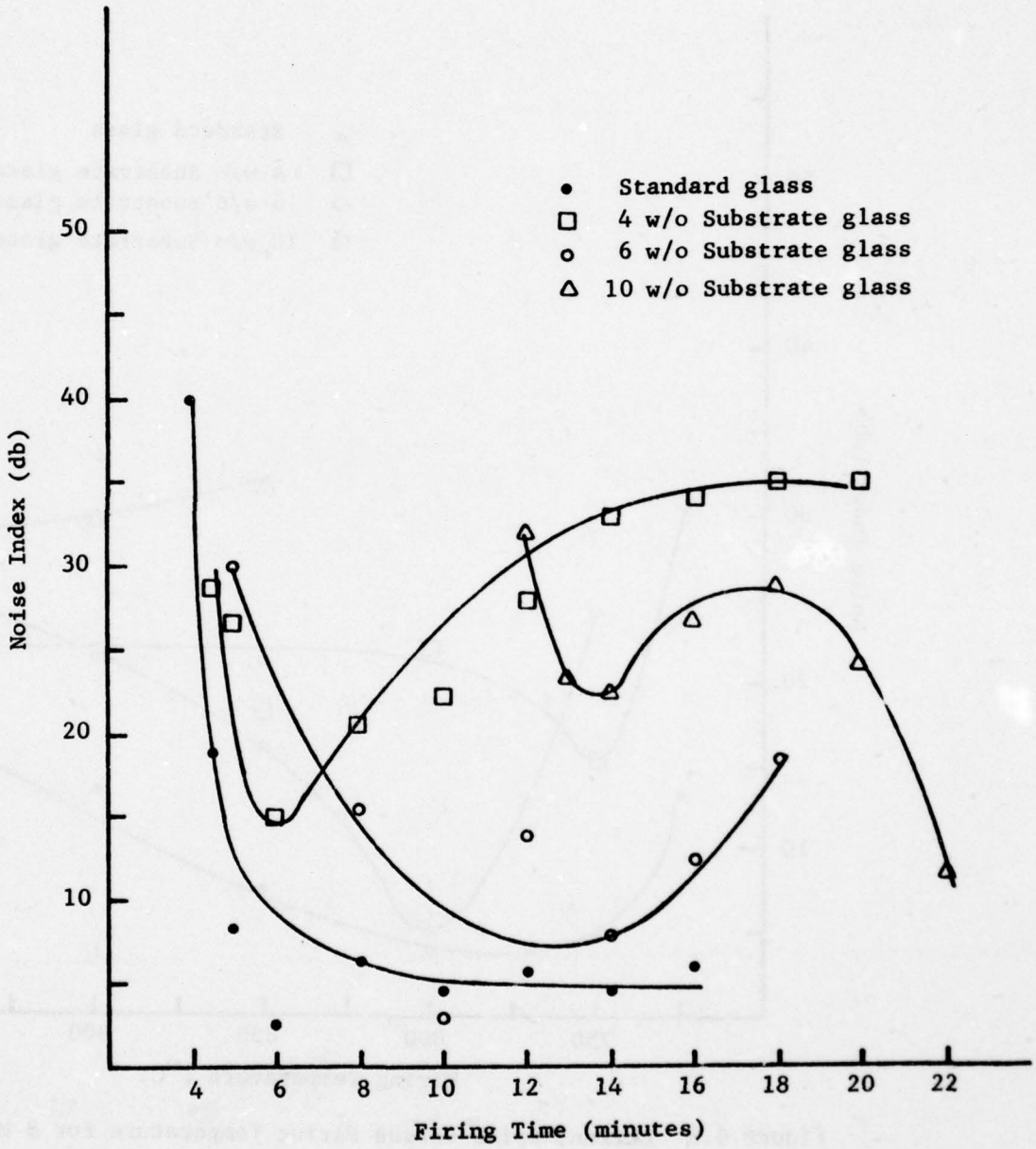

Figure 4.8. Current Noise versus Firing Time at 800°C.

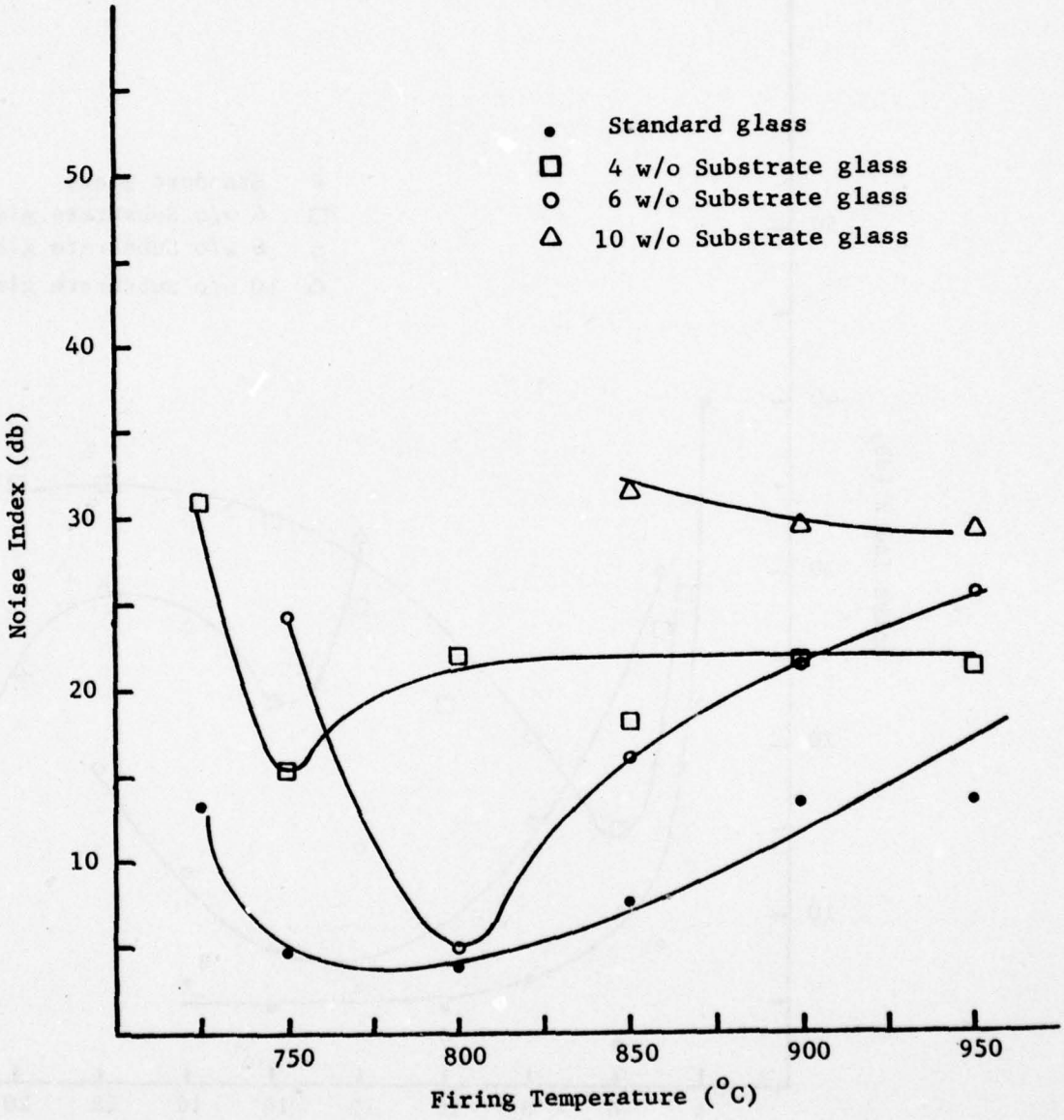

Figure 4.9 Current Noise versus Firing Temperature for 8 Minute Firing Time.

resistor chains, curves of NI vs. firing time or temperature should exhibit a decreasing noise index for increasing firing time/temperature as non-sintered contacts are converted to sintered ones. This decreasing characteristic is indeed observed in all eight curves during the initial stages of firing. As firing proceeds, the microstructure development model predicts a continued decrease in the noise index but at a slower rate. This type of behavior is exhibited by the standard glass resistors in Fig. 4.8 and the 10w/o substrate glass resistors in Fig. 4.9, but all other curves show a minimum followed by an increase in the noise index. The 10w/o substrate glass in Fig. 4.8 also shows a maximum followed by a second decrease in noise index. This anomaly has been associated with interactions at the resistor/conductor interface. The segregation problem, discussed in Section 4.1.1 in connection with choosing a conductive paste, will increase the number of non-sintered contacts in the vicinity of the electrodes thus increasing NI. Figures 4.10 through 4.13 are a series of photomicrographs of the interface between the conductor (dark region at the top of photomicrographs) and the resistor body after different firing times at 800°C. The standard glass resistors of Fig. 4.10 show signs of a decreasing density of the opaque RuO_2 relative to the transparent glass in the resistor near the conductor-resistor interface at short times (Fig. 4.10a), but a more uniform distribution of RuO_2 at longer firing times. The current noise for this type of resistor (Fig. 4.8) decreases rapidly at short times and remains fairly constant for firing times greater than 8 minutes. A very different behavior is seen with the 4w/o substrate glass resistors. In Fig. 4.11, a relatively uniform resistor/conductor interface is observed for short firing times, e.g., 4 and 6 minutes, but at longer firing times a thinning of the RuO_2 pigment in the resistor near the interface is observed. This

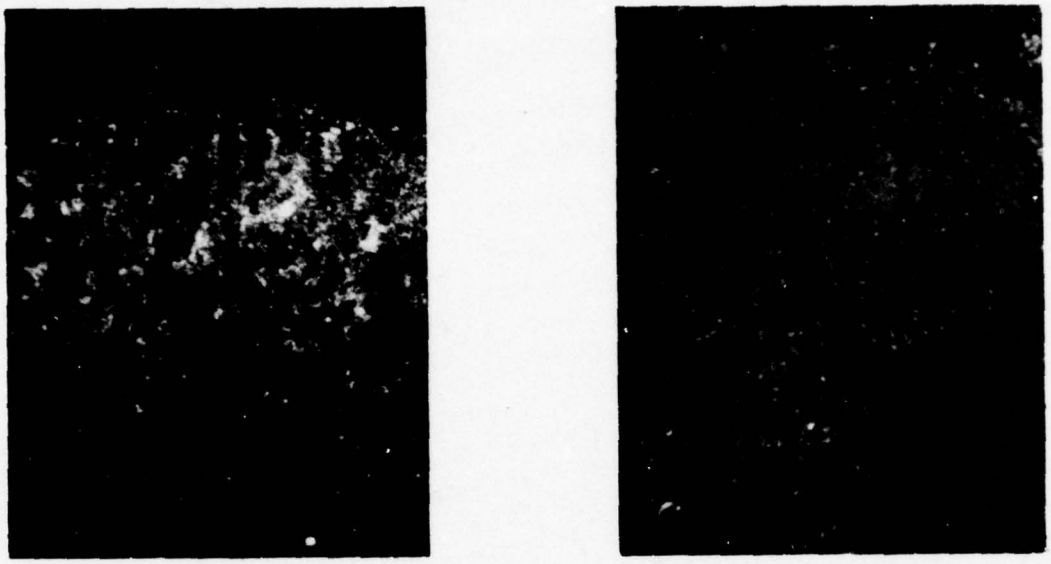

a. 3.5 minutes

b. 8 minutes

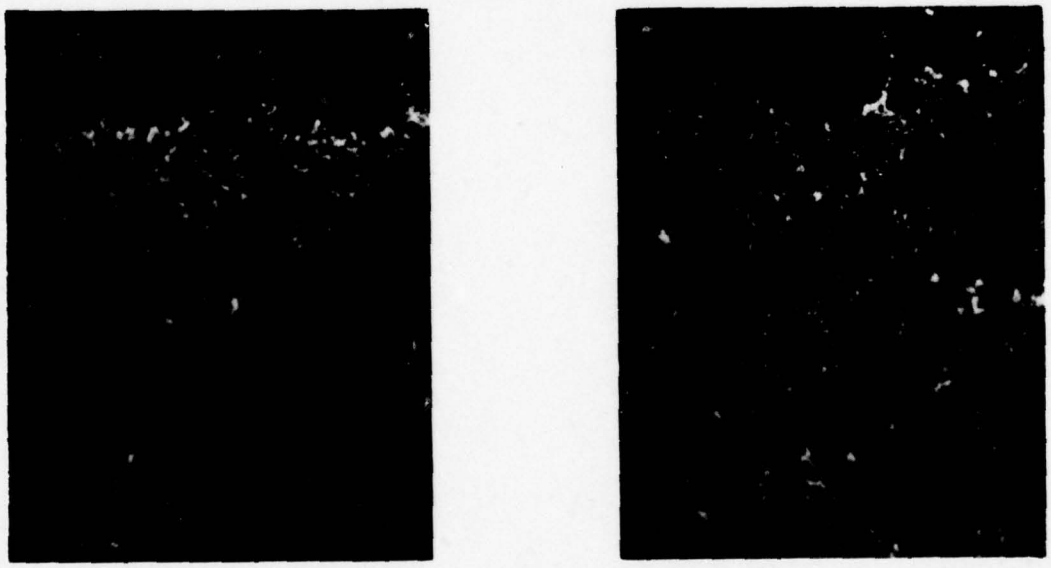

c. 12 minutes

d. 16 minutes

Figure 4.10. Resistor-Conductor Interface in Standard Glass Resistors Fired for Varying Times at 800°C.

a. 4 minutes

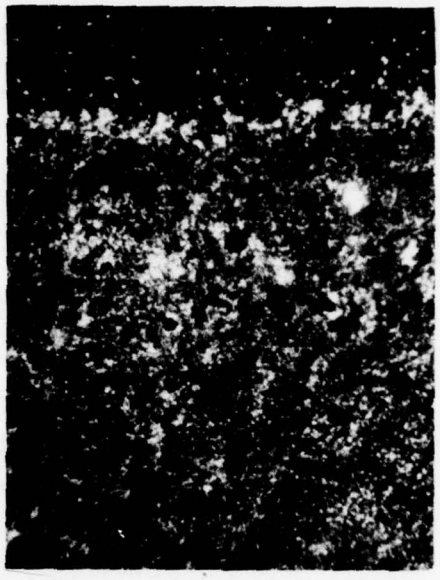

b. 6 minutes

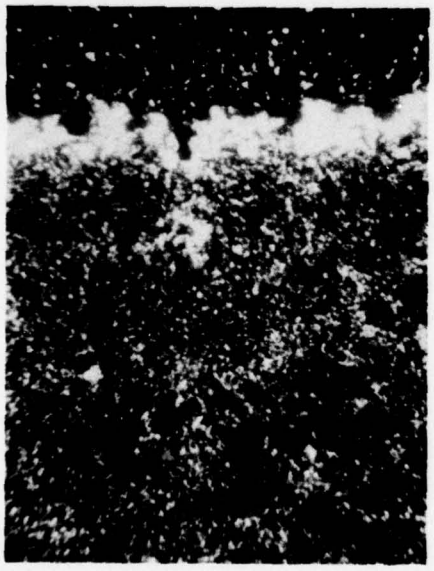

c. 10 minutes

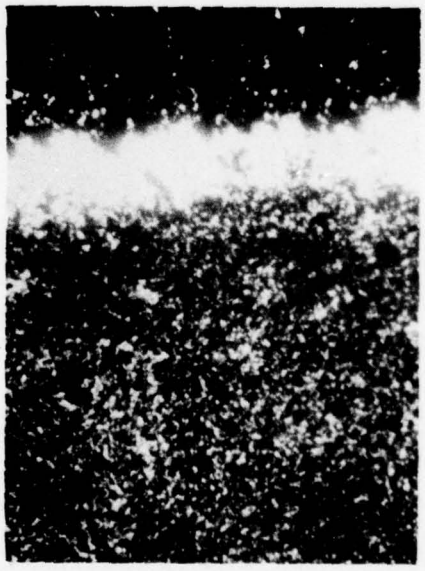

d. 14 minutes

Figure 4.11. Resistor-Conductor Interface in 4w/o Substrate Glass Resistors Fired for Varying Times at 800°C.

a. 4 minutes

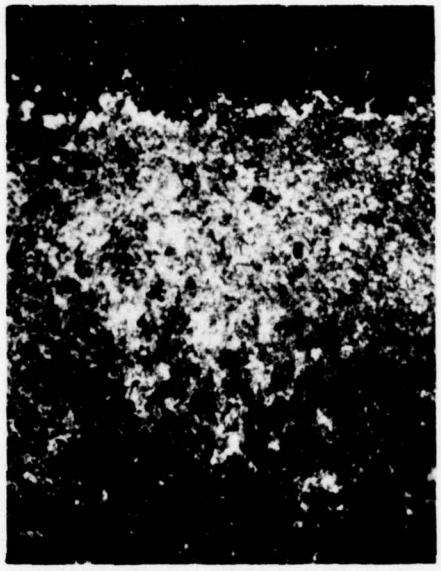

b. 6 minutes

c. 14 minutes

d. 18 minutes

Figure 4.12. Resistor-Conductor Interface in 6w/o Substrate Glass Resistors Fired for Varying Times at 800°C.

a. 10 minutes

b. 14 minutes

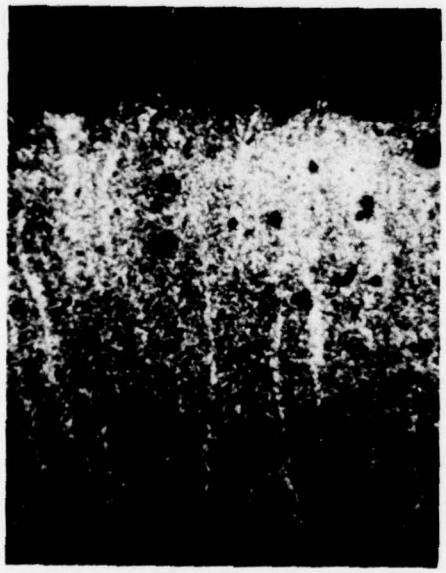

c. 18 minutes

d. 22 minutes

Figure 4.13. Resistor-Conductor Interface in 10w/o Substrate Glass Resistors Fired for Varying Times at 800°C.

segregation eventually reaches severe proportions after 14 minutes at 800°C (Fig. 4.11d), a firing condition which corresponds to the maximum in the current noise (Fig. 4.8). The 6 and 10w/o substrate glass resistors also show changes in the RuO_2 density near the resistor-conductor interface, as can be seen in Figs. 4.12 and 4.13. The 10w/o substrate glass resistors show a maximum in segregation near 18 minutes firing time with a more uniform RuO_2 density for both shorter and longer times, which correlates with the maximum in the noise index for this composition (Fig. 4.8).

The phenomenon of segregation at the resistor-conductor interface contributing to an increase in noise index has been observed by at least one other investigator. Stone [22] reported the same type of behavior in RuO_2 - lead borosilicate ($63PbO\text{-}25B_2O_3\text{-}12SiO_2$) glass resistors using a Du Pont platinum-gold 8895 conductive ink. Resistors containing 5, 7.5, and 10w/o RuO_2 were fired for a fixed time at varying temperatures and segregation was noted in all three inks from 700°C to 900°C. In each case, visual observation of the extent of RuO_2 thinning was correlated to a corresponding increase in noise index.

4.2 MIM Studies

4.2.1 Experimental

Metal-insulator-metal (MIM) devices were fabricated after several modifications in the originally proposed [7] experimental procedure. Sputtered platinum electrodes were found to be unsuitable due to fringing around the metal mask, which led to unacceptable pattern definitions. The electrode material was changed to evaporated gold in order to circumvent this problem. The substrate used with the modified procedure was an oxidized silicon wafer

coated with a layer of chromium prior to gold deposition in order to insure adequate adhesion. The glass was RF sputtered in a argon-oxygen atmosphere, and the top gold electrodes were evaporated in a dot pattern after the glass film had been annealed in oxygen.

The anneal step was necessary because it was possible that some of the PbO in the glass could have been reduced to elemental lead during the sputtering operation. In addition, stresses could have developed in the film due to the high energy impact between sputtered glass molecules and the existing film, and the density of the film may have been lower than that of bulk glass because of the sputtering deposition. Experiments to determine a proper temperature and time for annealing the sputtered films were carried out in an oxygen atmosphere, and temperatures were selected with reference to the results of studies of viscosity as a function of composition given in Section 3.1. The annealing point, defined as the temperature at which the viscosity is 10^{12} Pa·s, is 446°C for the standard glass; internal strains should be relieved in approximately 15 minutes at this temperature. The devices were annealed by placing the wafers in a fused quartz boat in a pyrex lined, resistively heated furnace at 380°C or 440°C with a constant flow of oxygen. The anneal times investigated were 30 minutes, 1, 2, 4, 6, and 8 hours accumulative, that is, a one hour anneal is the initial 30 minute anneal plus a second 30 minute anneal after electrical testing.

In order to compare the dielectric constant and conductivity of the sputtered film and bulk glass, parallel plate capacitors were made with the standard glass. A quantity of 63-25-12 glass was melted in a platinum crucible at 900°C and poured into a heated stainless steel mold. The mold was allowed to cool to room temperature, and the casting examined for cracks,

bubbles, or devitrification. Good quality glass blanks were then annealed at 450°C for 16 hours in air. A cylinder, 7.5 mm diameter, was cut from the blank using a diamond core drill, and the cylinder was sliced into 0.3 to 0.8 mm thick sections using a slow speed diamond saw. The samples were then polished and provided with evaporated gold electrodes.

The complex admittance and dissipation factor were measured as a function of frequency using a General Radio (GR 1615-A) capacitance bridge. The samples were placed on a vacuum chuck in a light tight, grounded metal box, and a micro-positioner with a tungsten probe was used to make contact to the lower electrode at a corner of the sample where the glass had been etched away. A second micro-positioner with a 76 μm gold wire was used to make contact to the top electrodes of the devices. All leads emerging from the metal box were coaxial cable. The GR 1615-A bridge measures either series capacitance (C_s) and dissipation factor (D) or the parallel capacitance (C_p) and parallel conductance (G_p). However, these quantities and the admittance (Y) are all interrelated through the following formulas.

$$Y = G_p + jwC_p \tag{4.4}$$

$$D = G_p/wC_p \tag{4.5}$$

$$C_s = (w^2C_p^2 + G_p^2)/w^2C_p \tag{4.6}$$

$$C_p = C_s/(1 + D^2) \tag{4.7}$$

$$G_p = wC_sD/(1 + D^2) \tag{4.8}$$

4.2.2 Results and Discussion

Figures 4.14 - 4.17 summarize the results from the anneal experiments. Figure 4.14 shows that the parallel capacitance and conductance both decrease

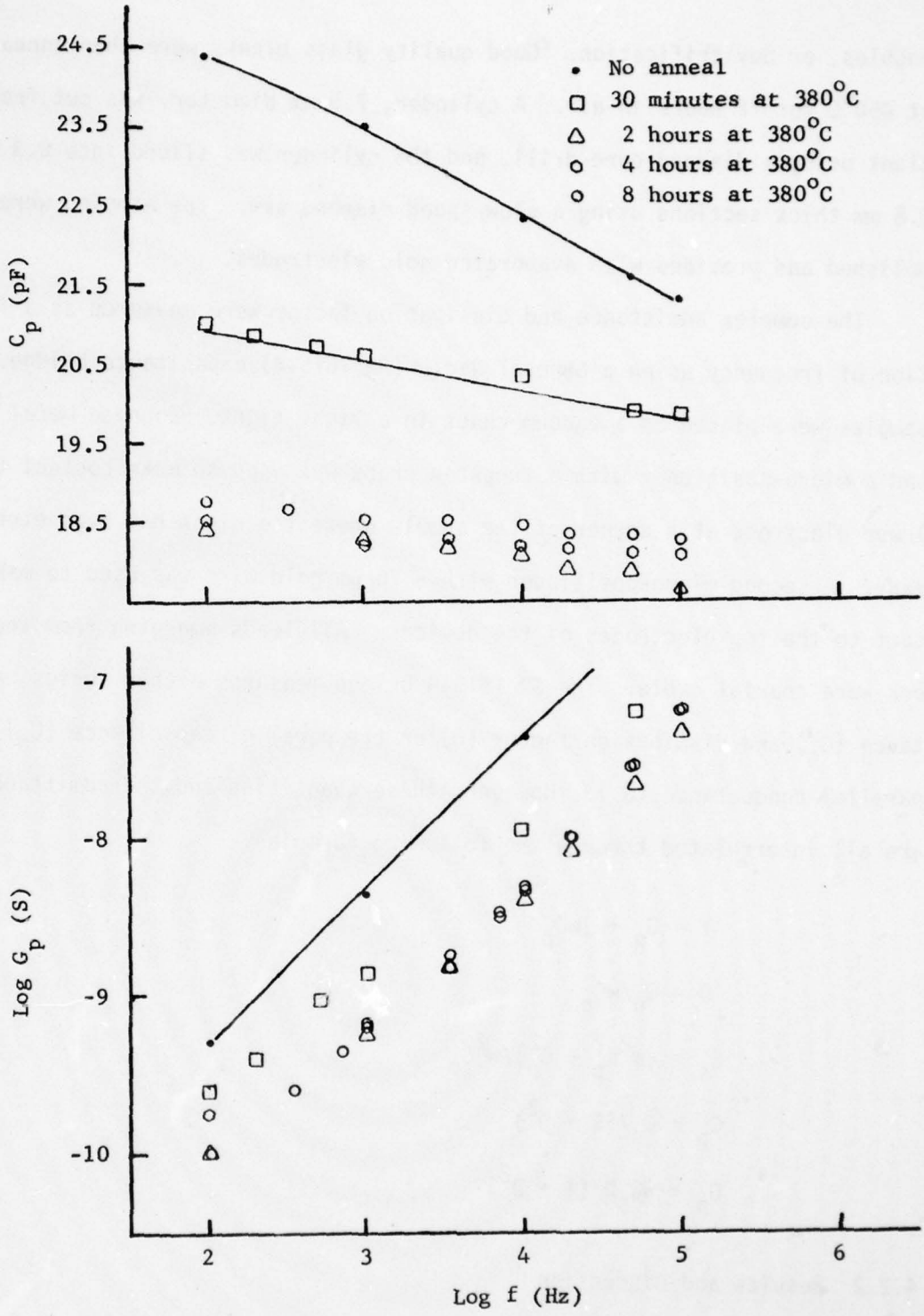

Figure 4.14. Parallel Conductance and Capacitance of MIM Devices with Standard Glass.

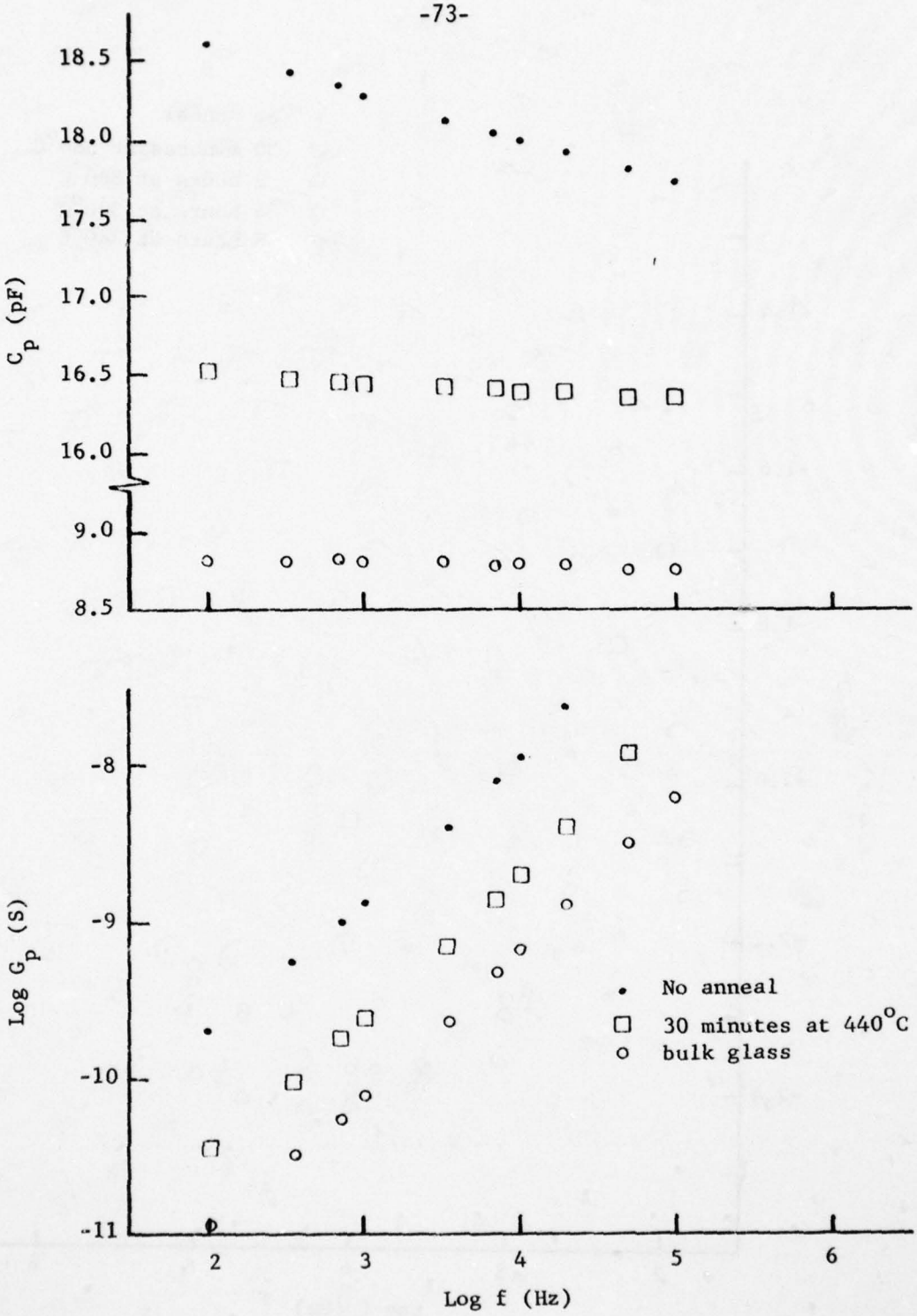

Figure 4.15. Parallel Conductance and Capacitance of MIM Devices and Bulk Standard Glass.

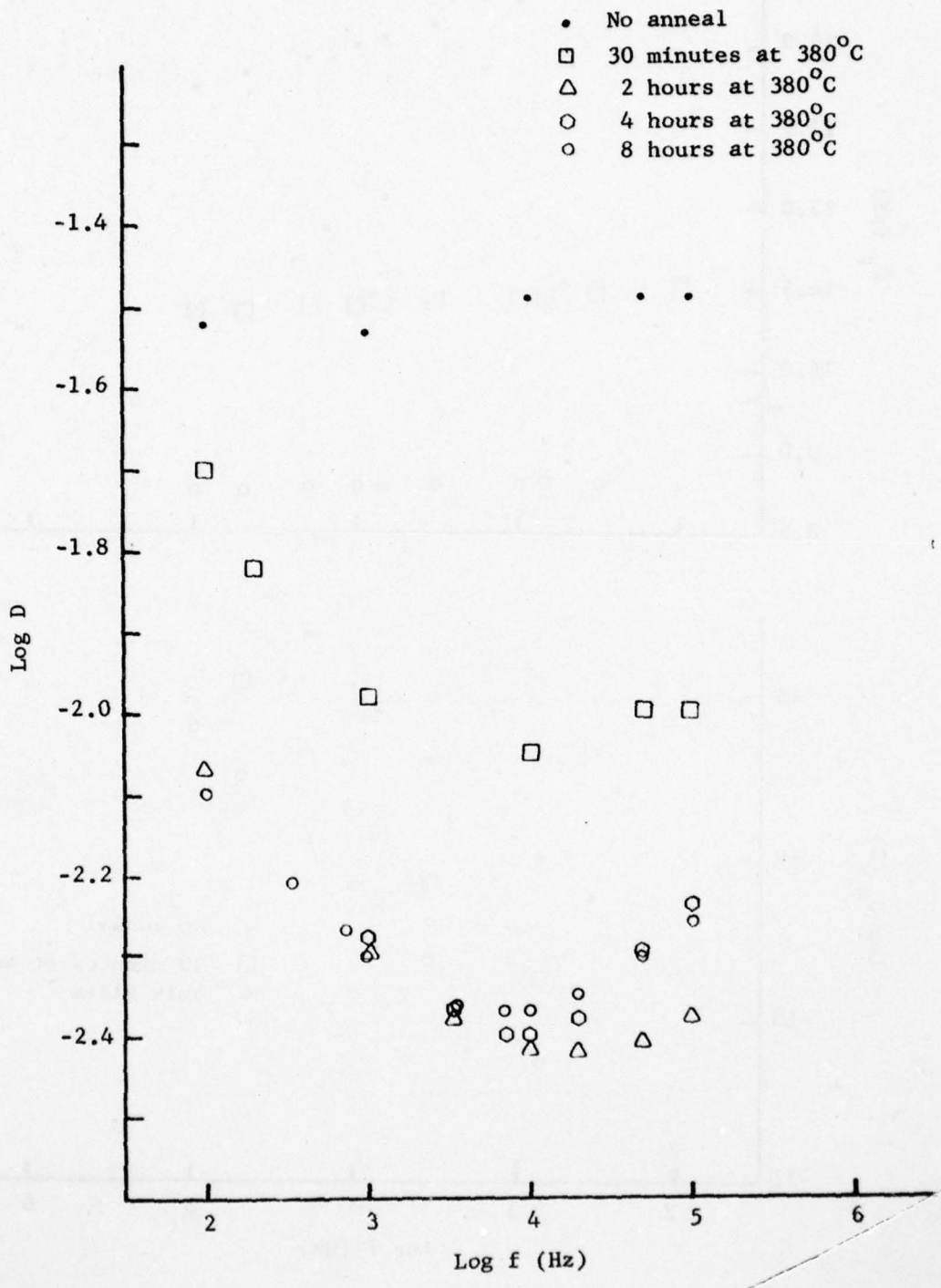

Figure 4.16. Dissipation Factor for Standard Glass MIM Devices Annealed at 380°C.

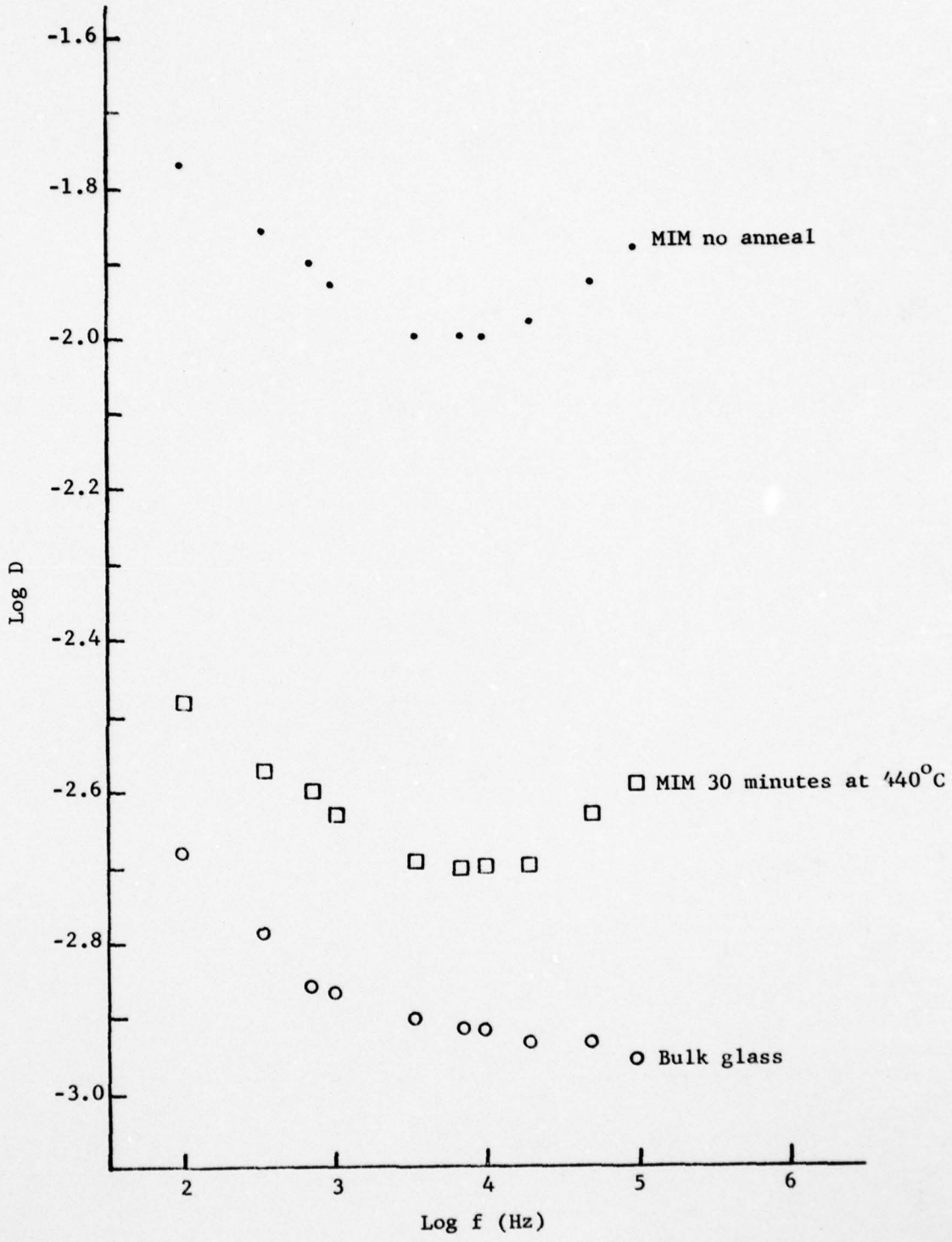

Figure 4.17. Dissipation Factor for Standard Glass MIM Devices and Bulk Standard Glass.

as the annealing time increases at 380°, but that little change occurs in either quantity after two hours of anneal. Figure 4.15 shows the parallel capacitance and conductance as a function of frequency for a virgin and an annealed MIM, and for a bulk glass sample which was also annealed at 440°C for 30 minutes. There is again a decrease in capacitance and conductance with annealing of the MIM device, and a decrease in the frequency dependence of C_p approaching the frequency independent behavior exhibited by the bulk glass sample. The dissipation factors corresponding to the data of Figs. 4.14 and 4.15 are plotted in Figs. 4.16 and 4.17 respectively. There is a suggestion of a minimum in the dissipation factor curves at approximately 10 kHz which may be indicative of a transition from a dissipation factor dominated by DC conductance, which would produce an inverse frequency dependence, to a dielectric loss mechanism which would produce a maximum at some higher frequency.

5. FUTURE WORK

Viscosity and surface tension as a function of glass composition and temperature will be measured at higher temperatures. The kinetics of ripening of RuO_2 in the glass will be determined as a function of glass composition and the kinetics of the initial stage of liquid phase sintering of RuO_2 will be calculated from the ripening data and the solubility data. These results will then be correlated utilizing the previously developed models for microstructure development, and the influence of glass composition established. The effects of substrate dissolution on charge transport processes in non-sintered contacts will be modeled, and the dependence of both the glass properties and the electrical properties of the non-sintered contacts on glass composition will be incorporated into a revised charge transport model for thick film resistors.

6. REFERENCES

1. A. Prabhu, G. L. Fuller and R. W. Vest, "Solubility of RuO_2 in a Pb Borosilicate Glass," J. Amer. Ceram. Soc., 57, 408 (1974).

2. A. Prabhu, G. L. Fuller, R. L. Reed and R. W. Vest, "Viscosity and Surface Tension of a Molten Lead Borosilicate Glass," J. Amer. Ceram. Soc., 58, 144 (1975).

3. A. Prabhu and R. W. Vest, "Investigation of Microstructure Development in RuO_2-Lead Borosilicate Glass Thick Films," Mater. Sci. Res., 10, 399 (1975).

4. R. W. Vest, "Development of Conductive Chains in RuO_2-Glass Thick Film Resistors," in Reactivity of Solids, Edited by J. Wood, et. al., pp. 695-699, Plenum Press, New York (1977).

5. R. W. Vest, "Conduction Mechanisms in Thick Film Mocrocircuits," Final Technical Report, Grant Nos. DAHC-15-70-G7 and DAHC-15-73-G8, ARPA Order No. 1641, December 1975.

6. R. W. Vest, "The Effects of Substrate Composition on Thick Film Circuit Reliability," Final Technical Report, Contract No. N00019-76-C-0354, February 28, 1977.

7. ibid, Contract No. N00019-77-C-0327, February 28, 1978.

8. A. R. Cooper, Jr., "Effect of Moving Boundary on Molecular Diffusion Controlled Dissolution or Growth Kinetics," Trans. Faraday Soc., 58, (480), pp. 2468-72 (1962).

9. J. Crank, Mathematics of Diffusion, pp. 104-105, Clarendon Press, Oxford, 1956.

10. A. R. Cooper, Jr. and W. D. Kingery, "Dissolution in Ceramic Systems: I. Molecular Diffusion, Natural Convection, and Forced Convection Studies of Sapphire Dissolution in Calcium Aluminum Silicate," J. Am. Ceram. Soc., 47 [1], pp. 37-43 (1964).

11. F. T. Trouton, "Coefficient of Viscous Traction and Its Relation to that of Viscosity," Proc. Roy. Soc. (London), 77, 426 (1906).

12. H. E. Hagy, "Experimental Evaluation of Beam-Bending Method of Determining Glass Viscosities in the Range 10^8 to 10^{15} Poises," J. Am. Cer. Soc., 46 (2), 93 (1963).

13. G. S. Fulcher, "Analysis of Recent Measurements of the Viscosity of Glasses," J. Am. Ceram. Soc., 8 (6), 339-55 (1925).

14. T. D. Taylor and G. E. Rindone, "Properties of Soda Aluminosilicate Glasses: V, Low-Temperature Viscosities," J. Am. Ceram. Soc., 53 (12), 692-5 (1970).

15. A. Abou-El-Azm and H. A. El-Batal, "Studies on the Softening Point of Some Borate Glasses Containing High Proportions of Lead Oxide in Relation to Their Structure," Physics and Chemistry of Solids, 10 (4), 159-63 (1969).

16. R. W. Vest, "Thick Film Glasses," Final Technical Report, Contract No. N00173-77-C-0142, November 15, 1978.

17. H. Fischmeister and G. Grimvall, "Ostwald Ripening - A Survey," Mater. Sci. Res., 6, 119 (1973).

18. J. Mukerji and S. R. Biswas, "Solubility of Ruthenium in Soda Silicate Glasses," Cent. Glass Cer. Res. Ins. Bull., 14, 30 (1967).

19. K. K. Dhasgupta and J. Mukerji, "Solubility Dependence of Ruthenium Volatilization from Glass," Trans. Ind. Cer. Soc., 27, 123 (1968).

20. C-T Tarn, unpublished research at Purdue University.

21. G. T. Conrad, Jr., N. Newman, and A. P. Stansbury, "A Recommended Standard Resistor-Noise Test System," IRE Trans. Comp. Parts, CP7 [3], 1-18 (1960).

22. K. E. Stone, "Current Noise in Thick Film Resistors," M.S. Thesis, Purdue University, May 1978.

DISTRIBUTION LIST

Naval Air Systems Command
Washington, D. C. 20361
Attn: AIR-310B (5 copies final)

AIR-360A
AIR-52022F
AIR-950D (14)

Director
Naval Research Laboratory
Washington, D. C. 20390
Attn: Dr. J. Murday (2)

Commander
Naval Avionics Facility
21st & Arlington Avenue
Indianapolis, Indiana 42618
Attn: Mr. D. Tague

Commander Naval Avionics Facility
21st & Arlington Avenue
Indianapolis, Indiana 42618
Attn: Mr. M. Cowart

Advisory Group on Electron Devices
201 Varick Street
New York, N.Y. 10014
Attn: Secretariat on LP Devices

Plessey, Inc.
20245 Sunburst Street
Chatsworth, CA 91311
Attn: Mr. E. Rogers

Westinghouse D & E Systems Center
P.O. Box 1897, M.S. 717
Baltimore, MD 21203
Attn: Dr. Ted Foster

Monsanto Research Corporation
Dayton Laboratory
1515 Nicholas Road
Dayton, Ohio 45477
Attn: Dr. R. Janowiecki

Director, ARPA
1400 Wilson Blvd.
Arlington, Virginia 22209
Attn: Dr. A. Bement

National Bureau of Standards
Bldg. 225, Rm. A-331
Washington, D. C. 20234
Attn: Mr. G. Harmon

Commander
Naval Electronics Laboratory Center
San Diego, CA 92152
Attn: Mr. O. Lindberg, Code 4800

Commander
Naval Weapons Center
China Lake, CA 93555
Attn: Dr. F. Essig, Code 601

Mr. Jack Ferrel
RADC/RBRM
Princeton, New Jersey 08540
Attn: Dr. T. Hitch (2)

Western Electric Engr. Research Center
Box 900
Princeton, New Jersey 08540
Attn: Dr. D. J. Shanefield
Dr. J. R. Piazza

Bell Laboratories
Allentown, PA 18103
Attn: Dr. H. Cohen
Dr. Y. Kim

Commanding Officer
AMSEL-TLIT
Fort Monmouth, New Jersey 07703
Attn: H. C. Frenkel

Hybrid Microcircuit Technology
Div. 2431
Sandia Laboratories
Albuquerque, NM 87115
Attn: Dr. R. K. Traeger (Div. 2431)
Dr. J. T. Grissom (Div. 2432)

Materials Research Laboratory
Department of Ceramic Science
Pennsylvania State University
University Park, PA 16302
Attn: Prof. J. V. Biggers

DISTRIBUTION LIST (Continued)

Reliability Analysis Center
Griffiss AFB, NY 13441
Attn: I. L. Krulac

State of the Art, Inc.
1315 South Allen
State College, PA 16801
Attn: Mr. D. Hamer

Thick Film Systems, Inc.
324 Palm Avenue
Santa Barbara, CA 93101
Attn: Mr. J. Provance

Rockwell International
Autonetics Division
Anaheim, CA 92803
Attn: J. Licari-Microcircuits

Commanding General
U.S. Army Electronics Command
Green Acres Bldg.
Ft. Monmouth, NJ 07703
Attn: J. Kelly-AMSEL-PP-1P1-1